Published for SISSA by Springer

Received: *July 11, 2024*
Accepted: *November 10, 2024*
Published: *January 8, 2025*

Search for diphoton resonances in the 66 to 110 GeV mass range using pp collisions at $\sqrt{s} = 13$ TeV with the ATLAS detector

The ATLAS collaboration

E-mail: atlas.publications@cern.ch

Abstract: A search is performed for light, spin-0 bosons decaying into two photons in the 66 to 110 GeV mass range, using 140 fb^{-1} of proton-proton collisions at $\sqrt{s} = 13$ TeV produced by the Large Hadron Collider and collected by the ATLAS detector. Multivariate analysis techniques are used to define event categories that improve the sensitivity to new resonances beyond the Standard Model. A model-independent search for a generic spin-0 particle and a model-dependent search for an additional low-mass Higgs boson are performed in the diphoton invariant mass spectrum. No significant excess is observed in either search. Mass-dependent upper limits at the 95% confidence level are set in the model-independent scenario on the fiducial cross-section times branching ratio into two photons in the range of 8 fb to 53 fb. Similarly, in the model-dependent scenario upper limits are set on the total cross-section times branching ratio into two photons as a function of the Higgs boson mass in the range of 19 fb to 102 fb.

Keywords: Beyond Standard Model, Hadron-Hadron Scattering, Higgs Physics

ArXiv ePrint: 2407.07546

https://doi.org/10.1007/JHEP01(2025)053

JHEP01(2025)053

Contents

1 Introduction

This paper presents a search for an additional light, spin-0 boson with an invariant mass ranging from 66 GeV to 110 GeV decaying into two photons, a signature that can arise in many theories of beyond the Standard Model (SM) physics. These include two-Higgs-doublet models (2HDMs) [1, 2] and next-to-2HDMs (N2HDMs) [3], next-to-minimal supersymmetric models (NMSSM) [4], and models of supersymmetry that introduce pseudo-Nambu-Goldstone bosons (R-axions) through symmetry breaking [5]. The introduction of an additional spin-0 boson can also be used to explain features observed in other experimental measurements. For example, the excess of GeV-scale gamma rays from the galactic centre can be explained if the additional spin-0 boson is a Higgs boson that acts as a scalar partner of dark matter [6]. Alternatively, if the additional spin-0 boson is an axion, even a weak coupling with the Higgs sector allows electroweak baryogenesis to explain the observed baryon asymmetry of the universe [7].

This analysis uses the full LHC proton-proton (pp) collision data sample at a centre-of-mass-energy of 13 TeV collected by the ATLAS detector (see section 2) during the years 2015–2018, corresponding to an integrated luminosity of 140 fb^{-1} at a centre-of-mass energy of 13 TeV. Both a model-independent search for a spin-0 particle (X) and a model-dependent search for an additional low-mass Higgs boson (H, assuming the production-mode cross-section times branching ratio into two photons as predicted by the SM at a given mass m_H) are performed. In both cases, the assumption of a narrow-width resonance (NWA) is

JHEP01(2025)053

made and interference effects between the signal and background processes are neglected. An additional search for larger-width signals is also performed in the model-independent search and considers ratios of decay widths Γ_X to the mass m_X of the spin-0 particle up to 2.5 %. Additional signal widths are not considered for the model-dependent analysis due to the narrow decay width of SM-like Higgs bosons in the mass range considered here [8].

Events that contain at least two photons (see section 3) are analysed for evidence of resonances in the diphoton invariant mass distribution. The diphoton final state provides a clean experimental signature due to the excellent invariant mass resolution of the ATLAS detector. In addition to the kinematic requirements, identification and isolation selections are applied to photons to reduce the impact of jet backgrounds and to ensure a high signal sensitivity (see section 4). The event selection, described in section 5, uses photon transverse energy E_T[1] selections that depend on the diphoton invariant mass $m_{\gamma\gamma}$ to suppress sculpting of the invariant mass distribution by the trigger selection. A gradient boosted decision tree (BDT) is additionally used for photon–electron discrimination.

Multiple event categories (see section 6) are defined to maximise signal sensitivity. The model-independent search for a spin-0 boson, X, splits the data into three categories based on whether the photons interact with nuclei in the detector that cause them to convert into a pair of electrons or not. Alternatively, the model-dependent search for an additional low-mass Higgs boson, H, employs a BDT to define three additional categories within each of the three photon-conversion categories, resulting in a total of nine categories. This additional categorisation is only used for the model-dependent result due to the SM-like production-mode cross-sections assumed for the signal sample used to train the BDT.

The resonant $m_{\gamma\gamma}$ signal distribution is modelled using analytic functions whose parameters are determined using Monte Carlo (MC) simulation, as described in section 7. There are two main components of the background: 1. the non-resonant $\gamma\gamma$, γj, and jj processes that are henceforth referred to as the *continuum background*, where "j" refers to a jet misidentified as a photon, and 2. the resonant *Drell-Yan* (DY) dielectron processes (mainly $Z \to ee$ events) in which both the electrons are misidentified as photons. The $m_{\gamma\gamma}$ distributions of both the background components are described by analytic functions determined from MC simulation and data-driven background estimations, further described in section 8. The uncertainty in the continuum background due to limited data and MC simulated events is reduced using a Gaussian Process regression [9]. The DY background affects prompt photons that convert to two electrons (converted photons) much more than those that do not (unconverted photons), hence a significant gain is obtained by splitting the analysis into separate conversion categories.

The final background $m_{\gamma\gamma}$ shape parameters, background yield, and potential signal yield are obtained from a fit to the diphoton invariant mass distribution in data. The $m_{\gamma\gamma}$ region 62 GeV to 120 GeV is chosen to minimise the systematic uncertainty in the background model. A search for hypothetical signal peaks in the range of 66 GeV to 110 GeV is performed,

[1] ATLAS uses a right-handed coordinate system with its origin at the nominal interaction point (IP) in the centre of the detector and the z-axis along the beam pipe. The x-axis points from the IP to the centre of the LHC ring, and the y-axis points upwards. Polar coordinates (r, ϕ) are used in the transverse plane, ϕ being the azimuthal angle around the z-axis. The pseudorapidity is defined in terms of the polar angle θ as $\eta = -\ln\tan(\theta/2)$ and is equal to the rapidity $y = \frac{1}{2}\ln\left(\frac{E+p_z c}{E-p_z c}\right)$ in the relativistic limit. Angular distance is measured in units of $\Delta R \equiv \sqrt{(\Delta y)^2 + (\Delta\phi)^2}$.

which ensures that there is enough data to constrain the background model both above and below the signal peak. The resulting p-value scans are presented in section 9. Since no significant excess is observed, limits are set on the cross-section times branching ratio within a fiducial volume defined at particle-level in the model-independent search for X and on the cross-section times branching ratio in the model-dependent search for H.

A previous search by the ATLAS Collaboration, using $20.3\,\text{fb}^{-1}$ of data at 8 TeV [10], found no significant excesses. Previous searches by the CMS Collaboration, using $19.7\,\text{fb}^{-1}$ of data at 8 TeV combined with $35.9\,\text{fb}^{-1}$ of data at 13 TeV [11], and later with $132.2\,\text{fb}^{-1}$ of data at 13 TeV [12], observed a maximal excess with a local (global) significance relative to the SM prediction of 2.8σ (1.3σ) at 95.3 GeV and 2.9σ (1.3σ) at 95.4 GeV, respectively.

2 ATLAS detector

The ATLAS experiment [13] at the LHC is a multipurpose particle detector with a forward-backward symmetric cylindrical geometry and a near 4π coverage in solid angle. It consists of an inner tracking detector surrounded by a thin superconducting solenoid providing a 2 T axial magnetic field, electromagnetic and hadronic calorimeters, and a muon spectrometer. The inner tracking detector covers the pseudorapidity range $|\eta| < 2.5$. It consists of silicon pixel, silicon microstrip, and transition radiation tracking detectors. Lead/liquid-argon (LAr) sampling calorimeters provide electromagnetic (EM) energy measurements with high granularity within the region $|\eta| < 3.2$. A steel/scintillator-tile hadronic calorimeter covers the central pseudorapidity range ($|\eta| < 1.7$). The endcap and forward regions are instrumented with LAr calorimeters for EM and hadronic energy measurements up to $|\eta| = 4.9$. The muon spectrometer surrounds the calorimeters and is based on three large superconducting air-core toroidal magnets with eight coils each. The field integral of the toroids ranges between 2.0 and 6.0 T m across most of the detector. The muon spectrometer includes a system of precision tracking chambers up to $|\eta| = 2.7$ and fast detectors for triggering up to $|\eta| = 2.4$. The luminosity is measured mainly by the LUCID–2 [14] detector, which is located close to the beampipe. A two-level trigger system is used to select events [15]. The first-level trigger is implemented in hardware and uses a subset of the detector information to accept events at a rate below 100 kHz. This is followed by a software-based trigger that reduces the accepted event rate to 1 kHz on average depending on the data-taking conditions. A software suite [16] is used in data simulation, in the reconstruction and analysis of real and simulated data, in detector operations, and in the trigger and data acquisition systems of the experiment.

3 Data and simulated event samples

The ATLAS detector was used to collect $\sqrt{s} = 13$ TeV pp collisions from the 2015–2018 LHC running periods, corresponding to an integrated luminosity of $139.5(12)\,\text{fb}^{-1}$ [17] after data-quality requirements [18]. The uncertainty in the integrated luminosity is obtained using the LUCID-2 detector [14] for the primary luminosity measurements, complemented by measurements using the inner detector and calorimeters. The data were recorded using diphoton triggers that required two EM clusters with transverse energies E_{T} above a certain threshold and satisfying identification criteria based on variables describing the shape of the

JHEP01(2025)053

EM showers in the calorimeter (hereafter called *shower shapes*) [19]. In the 2015 and the first portion of 2016 data taking, the E_{T} threshold was 20 GeV, while in the remainder of 2016 data taking $E_{\mathrm{T}} > 22$ GeV was required. During 2017 and 2018 data taking, the E_{T} threshold was reverted to 20 GeV, however an additional requirement on the sum of transverse energy around the photon candidate was applied [20].

Simulated event samples are used to study signal and background processes, and to determine the analytic functions used to model both. The search itself is performed by using the data to determine the parameters of the analytic functions (see section 8). Interference effects between the resonant signal and all background processes are expected to be small for the signal widths considered here [21] and are neglected.

Background events containing two photons with associated jets were simulated with the SHERPA 2.2.4 [22, 23] event generator. Matrix elements were calculated with up to three partons at next-to-leading order (NLO) in quantum chromodynamics (QCD) [24], and merged with the SHERPA parton shower [25] according to the ME+PS@NLO prescription [26]. The CT10 parton distribution function (PDF) set [27] was used in conjunction with dedicated parton shower tuning developed by the SHERPA authors. Events containing Z bosons decaying into electron pairs were generated at NLO in QCD using POWHEG BOX v2 [28, 29] interfaced to the PYTHIA 8.186 [30] parton shower model and the CT10 PDF set was used. The AZNLO set of tuned parameters for the underlying event [31] was used, with the CTEQ[6L1] PDF set [32]. Additional events containing Z bosons were also simulated with the SHERPA 2.2.1 event generator, for comparison with POWHEG BOX v2.

To better study electrons reconstructed as photons, single-electron and single-photon MC event samples were simulated with a pile-up profile corresponding to the Run 2 data sample. These single-particle samples were generated with transverse energy distributions covering the range from 5 GeV to 3 TeV.

The signal samples assume a SM Higgs boson at different mass values, and were generated at NLO in QCD using POWHEG BOX v2 interfaced to the PYTHIA 8.186 parton shower model using the AZNLO set of tuned parameters, for the gluon–gluon fusion (ggF) and vector-boson fusion (VBF) production modes. Samples were also simulated with the PYTHIA 8.186 event generator using the A14 set of tuned parameters [33], assuming the production of a Higgs boson in association with a W boson (WH), Z boson (ZH) or top-quark pair ($\mathrm{t\bar{t}H}$). Simulated samples were produced for fixed values of the mass of the assumed resonance, spanning the range 60 GeV to 120 GeV. Generally, the model-independent search for X uses the ggF sample as the nominal signal model with an uncertainty calculated by taking the envelope created by the other production modes, while the model-dependent search for a low-mass H combines all production modes for a given mass point assuming SM-like cross-sections. All assume a narrow-width resonance of 4 MeV that is negligible compared with the experimental resolution, which ranges from 0.9 GeV to 2.2 GeV (see section 7).

The effects of additional pp interactions in the same or neighboring bunch crossings (pile-up) were modeled by overlaying soft QCD processes simulated with PYTHIA 8.186 using the A2 set of tuned parameters [34] and the MSTW2008LO PDF set [35]. The simulated events are weighted to reproduce the distribution of average number of individual pp interactions per bunch crossing and the distribution of the primary vertex z-position observed in data (pile-up reweighting). All generated events were propagated through a detailed simulation of the ATLAS detector [36] based on GEANT [37]. The fast detector simulation used for background events containing two photons used a parameterisation of the performance of the calorimeters [38].

4 Event reconstruction

The event reconstruction is similar to the one described in ref. [39]. Photon candidates are reconstructed from topological clusters of energy deposited in the EM calorimeter (calorimeter clusters), and from charged-particle tracks and conversion vertices reconstructed in the ID. Photon clusters without any corresponding track in the ID are considered unconverted. Two opposite-charge tracks that form a vertex consistent with a massless particle and that both match to calorimeter clusters are considered converted photons; single-track vertices — essentially those without hits in the innermost ID layers — that match to a calorimeter cluster are also considered as converted photons [40]. Photon conversion fractions vary from 20 % to 65 %, depending on η [40]. Photons and electrons are required to fulfil identification criteria based on the shower shapes in the EM calorimeter [40]. Residual differences between the average values of the shower-shape variables measured in data and simulation using $Z \to \ell\ell\gamma$ events are corrected by shifting the shower-shape distributions in the simulation [41]. The photon identification efficiency is determined as a function of E_{T} and $|\eta|$ and the efficiency increases with E_{T} from 70% at 20 GeV to 90% at 50 GeV [19].

Photons are required to be in the high-precision EM calorimeter within the pseudorapidity interval $|\eta| < 2.37$, excluding the transition region $1.37 < |\eta| < 1.52$ between the barrel and end-cap calorimeters. Corrections to the energy of photon clusters is based on a multivariate regression algorithm optimised on simulated samples and scale factors derived extracted from data samples [42]. The two candidates with the highest transverse energies, both satisfying $E_{\mathrm{T}} > 22$ GeV, are retained. This transverse energy requirement is slightly higher than the trigger threshold, for most of the data-taking periods, to mitigate the trigger efficiency turn-on effect. A subsequent requirement on the ratio of photon E_{T} to the diphoton mass (see section 5) further raises the energy of selected photons. Primary vertices are reconstructed using at least two good-quality tracks with $p_{\mathrm{T}} > 500$ MeV [43]. The photon candidates are used to select the diphoton vertex using a neural-network algorithm based on charged-particle tracks and primary vertex information, as well as the direction of the two photons measured in the calorimeters and ID [44]. Once the diphoton vertex is selected, the direction of the two photon candidates is re-computed relative to this updated primary vertex. This recomputation improves the E_{T} measurement of each photon candidate through its dependence on the photon candidate's direction in η. The updated energy measurement improves the diphoton invariant mass resolution by about 8% for inclusive Higgs boson production relative to the default primary vertex selection [43].

Electron candidates — used for studying the DY background process — are reconstructed by matching tracks in the inner detector with clusters of energy deposits in the EM calorimeter formed with the same algorithm as in the photon reconstruction [40]. The tracks are required to be consistent with the diphoton vertex using their longitudinal (z_0) and transverse (d_0) impact parameters. Electrons must also satisfy the same E_{T} and η selection criteria as photons.

To improve the rejection of jets misidentified as photons, the candidates are required to be isolated using both the calorimeter and tracking detector information. The calorimeter-based isolation variable $E_{\mathrm{T}}^{\mathrm{iso}}$ is defined as the scalar sum of the E_{T} over positive-energy topological clusters [45] within a radius $\Delta R = 0.2$ around the photon candidate, excluding the photon energy and correcting for pile-up and underlying-event contributions [46–48]. For both the candidates this variable is required to be below $0.065 \times E_{\mathrm{T}}$, where E_{T} is the transverse energy of the photon. The track-based isolation variable $p_{\mathrm{T}}^{\mathrm{iso}}$ is based on charged-particle tracks, and is defined as the scalar sum of the transverse momenta p_{T} over tracks within a radius $\Delta R = 0.2$ around the photon candidate. Only tracks with $p_{\mathrm{T}} > 1\,\mathrm{GeV}$ that are consistent with originating from the diphoton production vertex and that are not associated with a photon conversion vertex are used. For both the candidates this variable is required to be below $0.05 \times E_{\mathrm{T}}$. Small differences between the average value of $E_{\mathrm{T}}^{\mathrm{iso}}$ between data and simulation are corrected in the simulation. The photon isolation efficiency — i.e., the fraction of photons fulfilling the identification requirement that also satisfy the isolation requirement — is determined using simulated samples and increases with $m_{\gamma\gamma}$ from 80 % at 62 GeV to 90 % at 120 GeV.

5 Event selection

Only events containing at least one primary vertex candidate are considered. The two selected photon candidates are used to define the diphoton invariant mass, $m_{\gamma\gamma}$, and only events in the mass range 62 GeV to 120 GeV are included in the analysis. To avoid distortions in the diphoton invariant mass spectrum due to the kinematic turn-on effects from the trigger selection, each photon is required to satisfy $E_{\mathrm{T}}/m_{\gamma\gamma} > 22/58 \approx 0.38$. This particular value is chosen to maximise the signal efficiency while allowing the mass range 62 GeV to 120 GeV to be described more easily using monotonically decreasing analytic functions (see section 8).

Following these selections, two significant background components are identified: $\gamma\gamma$, γj and jj continuum backgrounds coming from QCD production, and ee pairs coming from DY production. Here, the γj component includes events where either the leading or sub-leading object is a jet misidentified as a photon, and the jj component includes events where both the objects are jets misidentified as photons. The relative contribution of the continuum backgrounds varies by $m_{\gamma\gamma}$ and conversion category, with roughly 75 % due to $\gamma\gamma$, 20 % due to γj, and 5 % due to jj processes (see section 8). The contributions of events containing SM Higgs bosons or W and Z bosons produced in association with a photon are estimated by using MC simulated event samples and are found to be negligible.

To further reduce the number of background ee events, in particular the events where a topological cluster is ambiguously reconstructed as both an electron and a photon [40], a boosted decision tree (BDT) is developed using LightGBM [49]. Photon candidates from single-photon MC samples are considered as signal in the training, while photon candidates from the single-electron MC samples are considered as background when training the BDT. The model is trained using kinematic information related to the converted photon and detailed tracking information related to the electron and conversion of the photon candidate. The full list of variables considered for this classifier are chosen to avoid introducing shapes in the background distribution that are difficult to model with analytic functions (see section 8).

JHEP01(2025)053

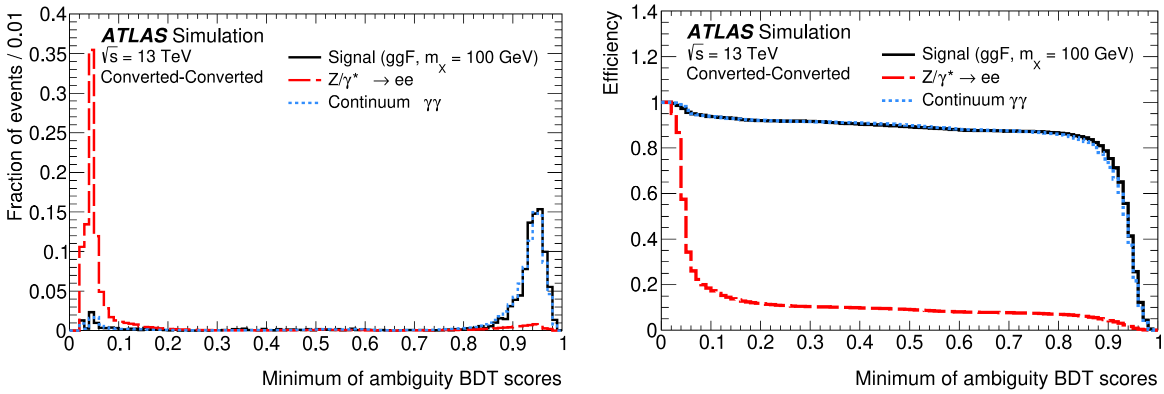

(a) (b)

Figure 1. (a) Distribution of electron–photon ambiguity BDT scores constructed by taking the minimum score of the two photon candidates in simulated ggF $m_X = 100\,\text{GeV}$ signal events (solid line), $Z/\gamma^* \to ee$ events (dashed line), and the continuum $\gamma\gamma$ background events (dotted line). The distributions are scaled independently for illustrative purposes. (b) Efficiency versus minimum requirement on the ambiguity BDT score, shown for the same samples. Only events in which both photon candidates are converted are shown.

The output of this classifier (henceforth referred to as the *ambiguity BDT*) is a score on the interval [0,1], where scores closer to 0 indicate an electron-like object and a score nearer to 1 indicate a photon-like object. Unconverted and non-ambiguous photons are assigned a score of 1 and are not further classified. The score of the ambiguity BDT is then evaluated for each of the two photon candidates. In figure 1, the minimum score between the two candidates and the selection efficiency for the signal and background processes are shown, both as a function of ambiguity BDT score in events with two converted photon candidates and thus most likely to suffer from ee backgrounds. Requiring both the ambiguity BDT scores to be above 0.2 results in a signal selection efficiency above 93 % and a reduction of ee backgrounds between 65 % to 90 %, where the largest reduction is obtained for events with two converted photons.

6 Event categorisation

As the ee backgrounds predominantly impact events where both photons convert to a pair of electrons (see section 4), including distinct conversion categories results in a significant increase in sensitivity to new physics. After the event selection from section 5 is applied, events are categorized into those where: 1. both photons remain unconverted (UU), 2. either one of the two photons convert (UC), or 3. both photons convert (CC).

For the model-dependent result, in addition to the conversion categories, events are separated between the continuum background and low-mass Higgs boson processes by another BDT, henceforth referred to as the *category BDT*. The training of this BDT is performed using the adaptive boosting (AdaBoost) algorithm [50], with a boosting parameter of 0.5, designed with the TMVA toolkit [51]. SM-like assumptions on the production-mode cross-sections are used for the model-dependent result. Eight input variables are considered and are given here ranked in order of variable importance in the training: the cosine of the difference in

Category	Selection Requirement
Model-Independent categories	
UU	2 unconverted photons
UC	1 converted photon and 1 unconverted photon
CC	2 converted photons
Model-Dependent categories	
UU1	UU and category BDT score < -0.2
UU3	UU and category BDT score $[-0.2,0)$
UU3	UU and category BDT score $>= 0$
UC1	UC and category BDT score < -0.2
UC2	UC and category BDT score $[0.2,0)$
UC3	UC and category BDT score $>= 0$
CC1	CC and category BDT score < -0.2
CC3	CC and category BDT score $[-0.2,0)$
CC3	CC and category BDT score $>= 0$

Table 1. The selection requirements and names of each category in the model-independent and model-dependent analyses.

azimuthal angle between the two photons, the ratio $E_{\mathrm{T}}/m_{\gamma\gamma}$ of each photon, the η of the each photon, the minimum of the two ambiguity BDT scores, and the ambiguity BDT scores of each of the two photons. Photon candidates from simulated samples with $m_H = 60$, 80, 100, and 120 GeV—where the different masses and production modes are weighted assuming the SM-like cross-sections for a Higgs boson at the specified m_H — are considered as signal (S) and simulated diphoton events are considered as background (B) when training this BDT. For simplicity, the photon candidates from all three conversion categories are used in the BDT training. The resulting category BDT score is shown in figure 2, for signal and background processes. The category BDT score is used to define three sub-categories within each of the three conversion categories, labelled as 1 to 3 in increasing order of expected signal compared to background. The nine categories are defined based on the combined conversion and BDT category as UU1, UU2, UU3, UC1, UC2, UC3, CC1, CC2, and CC3. The number of categories and the corresponding boundaries are optimised based on the expected signal-to-background significance, quantified by $S/\sqrt{B}$, while requiring that there are a sufficient number of simulated events for determining the background model. Each sub-category is required to contain at least 20% of the total number of diphoton background events in a given photon conversion category. While small differences in the optimal BDT score boundaries are found for different categories, for simplicity, the same boundaries in BDT score of -0.2 and 0 are used for all events. A list of each category and its requirements can be found in table 1.

The category BDT classification is found not to cause significant distortions of the diphoton invariant mass distribution for any category. The expected signal and background yields for a signal with $m_H = 90$ GeV are given in table 2.

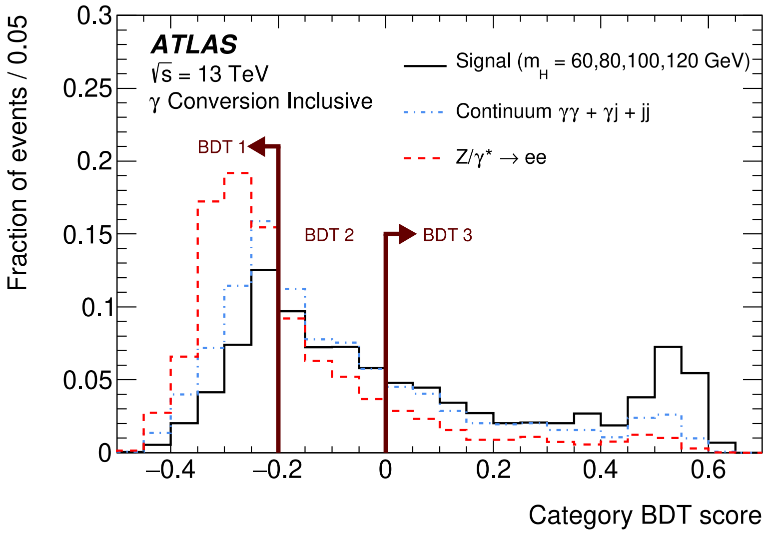

Figure 2. Distributions of the category BDT scores for the merged SM-like Higgs boson considering all production modes (ggF, VBF, $t\bar{t}$H, WH, ZH), the diphoton ($\gamma\gamma$) and reducible backgrounds (γj, jj) continuum, and the simulated $Z \to ee$ background prediction. The reducible background components are derived from dedicated data control regions where the photon identification and isolation requirements are inverted. The merged signal contains signals generated for $m_H = 60$, 80, 100, and 120 GeV and each MC sample is weighted according to the SM-like Higgs boson cross-section. Photons from all three conversion categories are used in the BDT training. The merged signal and backgrounds are separately normalised to unity. The vertical lines and arrows at category BDT scores of -0.2 and 0 define the categorisation used in this analysis. Events with category BDT scores below -0.2 are in BDT 1, events with category BDT scores between -0.2 and 0 are in BDT 2, and events with category BDT scores above 0 are in BDT 3.

BDT Category	SM-like Higgs boson ($m_H = 90$ GeV)						Background	
	Total	ggF [%]	VBF [%]	WH [%]	ZH [%]	$t\bar{t}$H [%]	Total [GeV^{-1}]	DY [GeV^{-1}]
1	741	97.1	1.2	1.0	0.6	0.1	18877	2179
2	942	93.4	2.9	2.1	1.2	0.4	14014	713
3	1187	72.4	13.5	6.7	4.0	3.4	6522	294
Total	2870	85.7	6.8	3.7	2.2	1.6	39413	3186

Table 2. The expected number of signal events, fractions of each Higgs boson production mode, and the number of background events per GeV at $m_{\gamma\gamma} = 90$ GeV for each BDT category, and for all three photon conversion categories together. The per GeV binning corresponds to approximately 1σ of the mass resolution at $m_{\gamma\gamma} = 90$ GeV. The background events are extracted from the background-only fit to the data and the "Total" category includes the number of Drell-Yan events (DY) that are also shown separately. The BDT categories are defined as follows: events with category BDT scores below -0.2 are in BDT category 1, events with category BDT scores between -0.2 and 0 are in BDT category 2, and events with category BDT scores above 0 are in BDT category 3.

JHEP01(2025)053

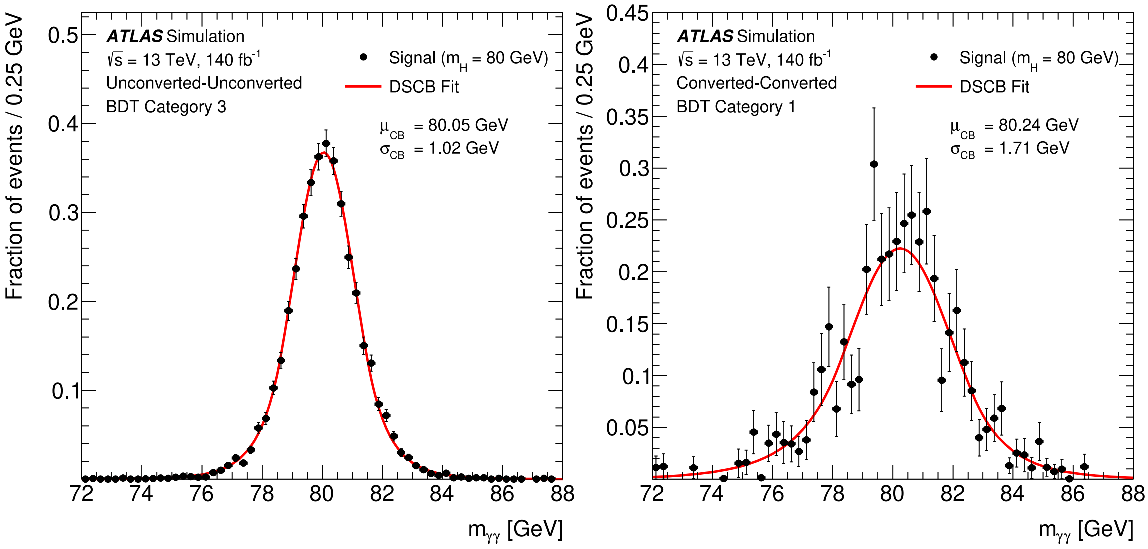

(a) (b)

Figure 3. Simulated diphoton invariant mass distribution of a narrow-width signal particle H of mass 80 GeV (points) in the (a) UU3 and (b) CC1 categories, overlaid with the DSCB function resulting from the signal model parameterisation (line). The error bars on the simulated data points indicate the statistical uncertainties. An arbitrary normalisation is used for illustration purposes.

7 Signal model

The $m_{\gamma\gamma}$ distribution of the signal, assumed to have a narrow decay width relative to the mass resolution, is modelled using a double-sided Crystal Ball (DSCB) function, composed of a Gaussian core with power-law tails [52, 53]. Each parameter is determined in a fit to the fixed-mass simulated samples, and is parameterised as a linear function of the resonance mass separately for each conversion category. For the model-independent search for a spin-0 scalar X only the ggF production mode is considered; for the model-dependent search for a low-mass H all production modes for a given mass value are combined assuming SM-like cross-sections [54]. The width of the Gaussian core, which is entirely determined by detector resolution, ranges from 0.9 GeV to 2.2 GeV depending on the resonance mass and analysis category. Good agreement between the signal model fit and the simulated $m_{\gamma\gamma}$ distribution is found, with reduced chi-square values generally between 0.9 and 1.4. Examples fits are illustrated in figure 3 for the UU3 and CC1 categories.

In addition to the narrow width signals considered above, a search for signals with larger widths is also performed in the model-independent analysis. The large width signal distributions for specific values of the mass and width are derived by convolving the detector resolution with the predicted line shape defined in the MC simulation of the ggF process. The detector resolution is modelled using the DSCB function described above and the signal line shapes are comprised of a Breit-Wigner (BW) function of width Γ_X combined with a mass-dependent gluon–gluon luminosity functional form. The large width signal hypotheses considered in this analysis cover the range $0\,\% \leq \Gamma_X/m_X \leq 2.5\,\%$. To ensure that sufficient side bands are available for the largest width signals, only signal masses in the range 75 GeV to 105 GeV are considered for the large-width analysis.

JHEP01(2025)053

8 Background estimate

The two main components of the background, the continuum and the resonant DY, are estimated separately in each category. In both cases, a data-driven approach is used to describe the normalisation and shape of their $m_{\gamma\gamma}$ distributions. The continuum background is fitted on data, with the normalisation and function parameters free. For the DY background, both the shape and normalisation are fitted, but the corresponding parameters are constrained using information from $Z \to ee$ decays, as described below.

The continuum background is predominately composed of events from $\gamma\gamma$ but also γj and jj production processes. To evaluate its composition, the two-dimensional side bands method described in ref. [55] is used to simultaneously extract the fraction of $\gamma\gamma$, γj, and jj events (including fake photons coming from DY electrons). The inputs to this method are the signal efficiencies of the identification and isolation requirements, as well as the number of events in sixteen categories, defined by whether each candidate passes or fails the photon identification and isolation criteria (four categories for each photon). The signal leakage in the background control regions — those that fail the photon identification or isolation requirements — is evaluated with simulation. A system of equations predicting the number of events in each category is solved with a χ^2 minimisation process, extracting the background decomposition estimate shown in table 3. The diphoton purity increases with the invariant mass $m_{\gamma\gamma}$ and varies from 60 % to 70 % across the mass range 62 GeV to 120 GeV with an uncertainty of 1 % to 5 % depending on the category. The uncertainties in this purity measurement arise from: statistical uncertainty in the data and simulated MC samples; the alternate definitions of the identification criteria that define the control regions; the dependence of the signal leakage evaluation in the control regions on the event generator; the modelling of the isolation variable and shower-shape distributions; and possible correlations between the isolation variables and the inverted identification criteria [55].

The continuum background $m_{\gamma\gamma}$ distribution in each category is described by an analytic function whose form is determined using the method described in ref. [56]. The bias related to the choice of analytic function is estimated as the fitted *spurious signal* [44] yield extracted using a signal-plus-background fit to a background-only template. The background-only template is built using simulated samples for the $\gamma\gamma$ component and a data control sample for the γj and jj components, mixed according to the fractions determined by the 2x2D side band method presented above. To minimise the effects of statistical fluctuations in the background-only template due to finite MC simulation statistics, the templates are smoothed with a Gaussian Process regression [9]. This analysis uses a similar methodology to that used in ref. [57], with an update to use the Gibbs kernel [58] to allow for an adaptive length scale hyperparameter. The following functions are considered: Bernstein polynomials [59] of order five to seven, and exponentials of second, third and fourth order polynomials. A function is only considered for modelling the background in a given analysis category if the maximal spurious signal from a fit to the background template is found to be less than 50% of the statistical uncertainty in the fitted signal yield (from the background distributions normalised to the same statistics as the data) over the mass range 66 GeV to 110 GeV. In the cases where two or more functions satisfy this requirement, the function with the fewest degrees of freedom is chosen to model the continuum background in that analysis category. For most

Category		UU	UC	CC
Model Independent	N_{data}	1356130	1104590	243984
	$f_{\gamma\gamma}$ [%]	74.4±1.3	69.2±3.3	61.6±3.7
	$f_{\gamma\text{j}}$ [%]	19.9±1.2	23.7±1.9	28.1±2.2
	f_{jj} [%]	5.3±0.5	6.0±0.7	7.3±1.7
	f_{DY} [%]	0.46±0.03	1.1±0.1	3.1±0.4
BDT Category 1	N_{data}	592403	494228	112603
	$f_{\gamma\gamma}$ [%]	71.5±2.0	67.0±3.4	57.3±3.8
	$f_{\gamma\text{j}}$ [%]	20.9±1.5	24.1±2.0	29.9±3.1
	f_{jj} [%]	6.8±0.6	7.2±0.9	8.2±0.9
	f_{DY} [%]	0.7±0.1	1.7±0.2	4.7±0.6
BDT Category 2	N_{data}	508548	401646	86275
	$f_{\gamma\gamma}$ [%]	74.7±1.4	69.7±4.1	64.5±3.8
	$f_{\gamma\text{j}}$ [%]	20.2±1.3	24.1±2.7	26.7±2.6
	f_{jj} [%]	4.8±0.5	5.5±0.6	7.0±1.2
	f_{DY} [%]	0.29±0.02	0.69±0.01	1.8±0.2
BDT Category 3	N_{data}	255179	208716	45106
	$f_{\gamma\gamma}$ [%]	80.4±1.0	73.5±2.8	66.6±5.1
	$f_{\gamma\text{j}}$ [%]	16.7±1.2	21.9±1.8	26.2±3.3
	f_{jj} [%]	2.7±0.3	4.0±0.9	5.5±1.4
	f_{DY} [%]	0.19±0.02	0.56±0.06	1.7±0.2

Table 3. The number of data events (N_{data}), the expected fraction of $\gamma\gamma$, γj, jj events determined with the two dimensional side band method, and the fraction of Drell-Yan events in each category. The uncertainties in the fractions of $\gamma\gamma$, γj, jj arise from the statistical uncertainty varying the identification requirements. The BDT categories are defined as follows: events with category BDT scores below -0.2 are in BDT Category 1, events with category BDT scores between -0.2 and 0 are in BDT Category 2, and events with category BDT scores above 0 are in BDT Category 3.

categories considered in this analysis, the result is an exponential of a third- or fourth-order polynomial. The exception is the UC category in the model independent analysis, which is modelled using a Bernstein polynomial of order six. The corresponding modelling uncertainty is derived by fitting the local maxima of the absolute spurious signal as a function of diphoton mass with an exponential of a second-order polynomial in each category.

The DY background is modelled using a DSCB function, with parameters determined by fitting a data-driven $m_{\gamma\gamma}$ template. At first order, this template is derived using an m_{ee} distribution from $Z \to ee$ events in data. Electrons are required to pass the same E_{T} and η requirements as photons, as well as identification requirements based on shower shape variables; no isolation requirement is applied. Because electrons misidentified as photons

JHEP01(2025)053

generally lose a large amount of energy due to bremsstrahlung, a Smirnov transformation [60] derived from simulation is used to correct the m_{ee} template shape to the $m_{\gamma\gamma}$ shape expected from electrons faking a photon. The normalisation of the resulting $m_{\gamma\gamma}$ template is computed from $e \to \gamma$ fake rates obtained from the same data used to derive the template, as described in ref. [10], and is shown in table 3. Since electrons reconstructed as unconverted photons are more affected by bremsstrahlung than those reconstructed as converted photons, the UU events are more shifted to lower invariant masses than CC events. To account for these differences, the Smirnov transformation and normalisation are derived separately for each analysis category. Variations arising from limited MC sample sizes, variations of the Z-boson mass window and background subtraction used when deriving fake rates, results using different MC event generators, and results using different detector geometries are considered as uncertainties.

9 Results

For the model-independent result, the measurement of the signal production cross-section times branching ratio, $\sigma_{\text{fid}} \times \mathcal{B}$, is performed in a fiducial region. The fiducial region, which closely matches the selection requirements of the reconstructed photons, is constructed in order to reduce the dependence of the measurement on the chosen theoretical model. The fiducial region is defined at particle level as: two photons with $E_{\text{T}} > 22\,\text{GeV}$, $|\eta| < 2.37$ excluding $1.37 < |\eta| < 1.52$, passing the isolation requirement $E_{\text{T}}^{\text{iso}} < 0.065\ E_{\text{T}} + 1\,\text{GeV}$, and passing $E_{\text{T}}/m_{\gamma\gamma} > 22/58$. Here, $E_{\text{T}}^{\text{iso}}$ is defined as the magnitude of the vector sum of p_{T} for all particles with a lifetime longer than 10 ps (except neutrinos and muons) within a radius of $\Delta R = 0.2$ around the photon. This isolation requirement is chosen to reproduce the detector-level selection. The particle-level fiducial cross-section includes a signal efficiency correction factor C_X through:

$$\sigma_{\text{fid}} \times \mathcal{B} = \frac{N_{\text{S}}}{C_X \mathcal{L}}, \text{ with } C_X = \frac{N_{\text{MC}}^{\text{det}}}{N_{\text{MC}}^{\text{fid}}}, \tag{9.1}$$

where N_{S} is the fitted number of signal events in data, $\mathcal{L}$ is the integrated luminosity, $N_{\text{MC}}^{\text{det}}$ is the number of simulated signal events passing the detector-level selection criteria, and $N_{\text{MC}}^{\text{fid}}$ is the number of simulated signal events passing the particle-level selection. Since a generic spin-0 scalar X is targeted, only the ggF production mode is used for the nominal correction factor, and the C_X factor values range from 0.46 to 0.69 as a function of m_X. The envelope of the C_X values from the five production modes is taken as an uncertainty. This model dependence uncertainty is determined using simulated samples of X with several production modes: ggF, VBF, VH, and $\text{t}\bar{\text{t}}\text{H}$.

Several experimental uncertainties directly impact the signal yields and signal shape and are accounted for in the fit using nuisance parameters constrained by Gaussian penalty terms in the likelihood function. The largest effect on the signal yield in the model-dependent analysis comes from the uncertainty in the pile-up reweighting procedure. This uncertainty is estimated by changing the nominal rescaling factor and evaluating the change in the signal efficiency. Uncertainties in the signal yield arising from uncertainties in the luminosity determination, the trigger efficiency, and photon identification and isolation efficiencies are also considered. Uncertainties in the signal mass scale and resolution are assessed by propagating the photon energy calibration uncertainties onto the MC signal samples and constructing a new signal template. These shifted signal templates are then refit using the signal model parameterisation given in section 7 and the deviations from the central mass and resolution values are taken as an uncertainty. These uncertainties in the signal mass scale (resolution) are in the range ±0.3 % to ±0.5 % (±3 % to ±10 %), with the larger uncertainties occurring at higher values of $m_{\gamma\gamma}$. A systematic uncertainty is derived from the variation of the detector material description in the simulation, resulting in migrations across conversion categories. An uncertainty is also assessed on the electron-photon ambiguity BDT efficiency that accounts for differences in performance between data and the MC simulation selection efficiency in a control region outside of the mass range considered in this analysis. The absolute differences in efficiencies between data and MC simulation are found to be 0.1 %, 1.2 %, and 2.9 % for the UU, UC, and CC categories, respectively. Since no attempt was made to remove the γj and jj components from the diphoton data samples — accounting for around the 25 % of the data sample in the mass range 110 GeV to 120 GeV—these differences are expected to be conservative estimates. The envelope of these uncertainties results in an uncertainty of 0.7 % on the signal selection efficiency. The variations on the DY background result in uncertainties in the peak position, the peak width, and the normalisation which are derived separately for each conversion category. The magnitude of these uncertainty components is shown in table 4.

For the model-dependent result, the total signal production cross-section times branching ratio, $\sigma_{\mathrm{H}} \times \mathcal{B}$, is computed as:

$$\sigma_{\mathrm{H}} \times \mathcal{B} = \frac{N_{\mathrm{S}}}{A_H C_H \mathcal{L}}, \tag{9.2}$$

where N_S is the number of signal events fit in data, C_H is the signal efficiency factor for a SM-like Higgs boson, and A_H is an acceptance factor defined as the probability of a generated event to be selected in the fiducial volume at the particle level. The A_H and C_H factors are parameterised using the weighted average of the different Higgs boson production modes assuming the SM-like cross-section for each production mode. The acceptance times correction factor varies from 0.13 to 0.2 depending on the mass of the SM-like Higgs boson m_H. Since the model-dependent result assumes SM-like production-mode cross-sections when constructing C_H, the uncertainty from taking the envelope of the production modes — as done when deriving C_X in the model-independent results — is not relevant. After accounting for the differences between the analyses, the model-dependent result provides an approximately 30 % to 60 % stronger limit than the model-independent result.

The expected fraction of signal events for the model-independent (model-dependent) analysis in each of the three conversion (nine) categories is parameterised as a function of m_X (m_H). The migration of signal events between different BDT categories in the model-dependent analysis is found to be negligible.

The number of signal and background events is measured with an extended maximum-likelihood simultaneous binned fit to the $m_{\gamma\gamma}$ spectra. This fit is performed in the three conversion categories for the model-independent analysis and in nine categories (three BDT categories for each conversion category) in the model-dependent analysis. Scans over different

JHEP01(2025)053

m_X and m_H hypotheses are performed in 0.1 GeV steps over the mass range 66 GeV to 110 GeV.

The signal-plus-background model has the form:

$$N_S \cdot f_S(m_{\gamma\gamma}) + N_{SS} \cdot f_S(m_{\gamma\gamma}) + N_B \cdot f_B(m_{\gamma\gamma}) + N_{DY} \cdot f_{DY}(m_{\gamma\gamma}), \tag{9.3}$$

where f_S is the signal model described in section 7, N_S (N_B) is the fitted number of signal (continuum background) events, N_{SS} is the number of spurious signal events, f_B (f_{DY}) is the continuum (Drell-Yan) background model described in section 8, and N_{DY} is the number of DY background events. The systematic uncertainties are included in the likelihood via nuisance parameters, and constrained by Gaussian or log-normal penalty terms.

A background-only fit of the data is shown in figure 4 for the three model-independent conversion categories and in figure 5 for the three model-dependent BDT 3 categories. The parameters of the background model in each category are determined during a simultaneous fit to all categories. A goodness-of-fit test is performed in each category and returns a probability between 5% and 89% depending on the category. As expected, the DY contribution is most prominent in the CC categories (see table 3).

The compatibility of the observed diphoton mass spectra with the background-only hypothesis, for a given resonance mass, is determined with a local p-value based on the profile-likelihood-ratio-test statistic [61] as detailed in ref. [53]. The observed and expected 95 % confidence level (CL) exclusion limits on the production cross-section times branching ratio are evaluated using a modified frequentist approach $\mathrm{CL_s}$ [62] with the asymptotic approximation to the test-statistic distribution [61].

The result of the model-independent p-value scan is shown in figure 6(a). No significant excess with respect to the background-only hypothesis is observed. The largest localised deviation for the model-independent search is observed for a mass of 71.8 GeV, corresponding to a local significance of 2.2σ.

For the narrow-width model-independent result, an upper limit at the 95 % CL is set on $\sigma_{\text{fid}} \times \mathcal{B}$ from 8 fb to 53 fb, as shown in figure 6(b).

The model-independent analysis considers additional larger width signal hypotheses, and the p-value scan is expanded to include signal hypotheses with Γ_X/m_X in the range 0 % to 2.5 %. The result of this p-value scan is shown in figure 7. Due to the truncated range in m_X, the most significant excess occurs at 85.2 GeV for the narrow-width model hypothesis and corresponds to a local significance of 1.7σ. In the absence of a significant excess, upper limits are set on $\sigma_{\text{fid}} \times \mathcal{B}$ as a function of Γ_X/m_X and are illustrated in figure 8.

The result of the model-dependent p-value scan is shown in figure 9(a) and the largest deviation is observed for a mass of 95.4 GeV, corresponding to a local significance of 1.7σ. An upper limit at the 95 % CL is set on $\sigma_H \times \mathcal{B}$ from 19 fb to 100 fb for the model-dependent result, as shown in figure 9(b). The limited number of pp collisions recorded is the dominant uncertainty impacting this result. The model-dependent result can be compared to a similar result from the CMS Collaboration, which sets an observed upper limit ranging from 15 fb to 73 fb in the mass range 70 GeV to 110 GeV [12]. The largest deviation observed by CMS is for a mass of 95.4 GeV, corresponding to a local significance of 2.9σ.

JHEP01(2025)053

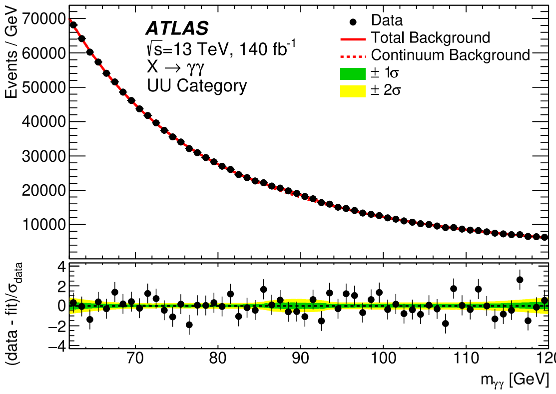

(a)

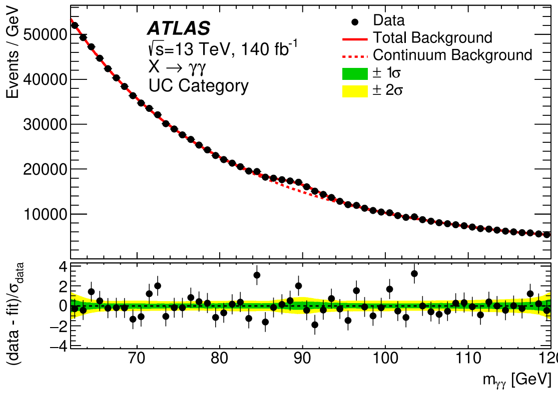

(b)

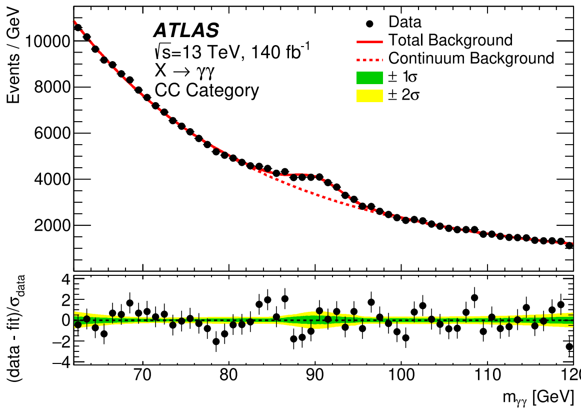

(c)

Figure 4. Background-only fit to the data (black markers) as a function of the diphoton invariant mass $m_{\gamma\gamma}$ for the model-independent conversion categories: (a) UU, (b) UC, and (c) CC. The solid lines show the sum of the Drell-Yan and the continuum background components and the dashed lines show only the continuum background components. The difference between the data and the total background component divided by the statistical uncertainty of the data, σ_{data}, is shown at the bottom panel separately for each category. The green (yellow) bands denote the total uncertainty in the background model at one (two) standard deviation.

Despite using the same *pp* collision events, the results between the model-dependent and model-independent searches in this analysis are expected to show differences due to the model assumptions and additional categories used in the model-dependent analysis. An example that illustrates these differences is the mild excess of events that appears around $m_H = 77\,\mathrm{GeV}$ in the model-dependent analysis. This mild excess is localised in two high-significance categories, UU3 and UC3, which contain about 20 % of all UU and UC events. In the low-significance categories that comprise the bulk of the UU and UC events, a deficit of events is observed, which matches that observed in the model-independent analysis.

JHEP01(2025)053

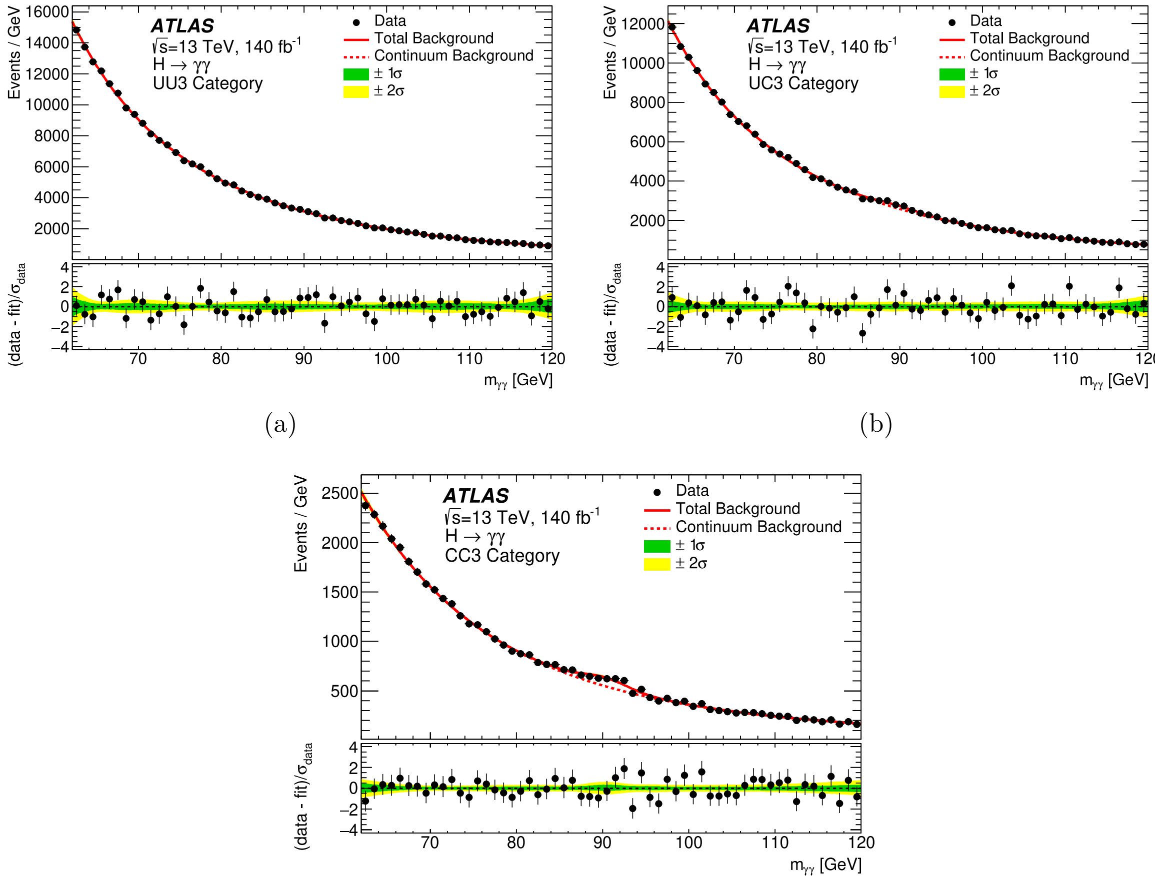

(a) (b) (c)

Figure 5. Background-only fit to the data (black markers) as a function of the diphoton invariant mass $m_{\gamma\gamma}$ for each of the model-dependent BDT 3 categories: (a) UU3, (b) UC3, and (c) CC3. The solid lines show the sum of the Drell-Yan and the continuum background components and the dashed lines show only the continuum background components. The difference between the data and the total background component divided by the uncertainty, with σ_{data} denoting only the statistical error of the data, is shown at the bottom panel separately for each category. The green (yellow) bands denote the total uncertainty in the background model at one (two) standard deviation.

10 Conclusion

Searches for new narrow-width resonances, either a generic spin-0 particle or an additional low-mass Higgs boson, are performed in the diphoton invariant mass spectra ranging from 66 GeV to 110 GeV, using 140 fb^{-1} of *pp* collision data collected at $\sqrt{s} = 13\,\text{TeV}$ with the ATLAS detector at the Large Hadron Collider. The dominant uncertainties arise from the limited number of *pp* collisions collected and the spurious signal uncertainty due to the choice of analytic functions to model the continuum background. Both a model-independent search for a spin-0 particle (X) and a model-dependent search for an additional low-mass Higgs boson (H, assuming the SM production-mode times branching ratio to two photons cross-sections) are performed. No significant excess above the SM background expectation is observed, and 95 % CL upper limits on the cross-section times branching ratio are set for each

JHEP01(2025)053

Source	Uncertainty [%]	Remarks
		Signal yield
Luminosity	±0.83	
Electron-photon ambiguity BDT efficiency	±0.7	
Trigger efficiency	±1.0 – 1.5	m_X-dependent
Photon identification efficiency	±1.8 – 3.0	m_X-dependent
Photon isolation efficiency	±1.6 – 2.4	m_X-dependent
Photon energy scale	±0.1 – 0.3	m_X-dependent
Photon energy resolution	±0.1 – 0.15	m_X-dependent
Pile-up	±1.6 – 5.0	m_X-dependent
Production mode	±4.3 – 29	m_X-dependent (model-independent only)
		Signal modelling
Photon energy scale	±0.3 – 0.5	m_X- and category-dependent
Photon energy resolution	±3 – 10	m_X- and category-dependent
		Migration between categories
Material	−2.0 / +1.0 / +4.1	category-dependent
		DY background modelling
Peak position	±0.1 – 0.2	category-dependent
Peak width	±1.9 – 3.5	category-dependent
Normalisation	±7.1 – 13	category-dependent
		Continuum background (model-dependent)
Spurious signal, NWA	9 – 171 events, (10% – 50%)	m_X- and category-dependent
		Continuum background (model-independent)
Spurious signal, NWA	37 – 310 events, (20% – 50%)	m_X- and category-dependent
Spurious signal, $\Gamma_X/m_X = 1.0\%$	65 – 539 events, (20% – 50%)	m_X- and category-dependent
Spurious signal, $\Gamma_X/m_X = 2.5\%$	92 – 879 events, (20% – 50%)	m_X- and category-dependent

Table 4. Summary of the systematic uncertainties considered in this analysis. In general, the values correspond to the uncertainties associated to the fit nuisance parameters. The DY uncertainty is the percent error on the nominal peak position, peak width, and normalisation. The spurious signal uncertainty is expressed as a number of events and relative to the expected statistical uncertainty (δS) of a fitted signal. The "Remarks" column indicates specific information about the systematic uncertainty, including whether or not the uncertainty varies as a function of resonance mass or analysis category.

search. In the model-independent analysis, the observed 95 % CL upper limits on the fiducial cross-section times branching ratio for a generic spin-0 signal are in the range 8 fb to 53 fb for new resonances with masses $66 < m_X < 110$ GeV. For the model-dependent analysis, the observed upper limits on the production cross-section times branching ratio to two photons for a SM-like Higgs boson range from 19 fb to 102 fb in the same mass range.

Acknowledgments

We thank CERN for the very successful operation of the LHC and its injectors, as well as the support staff at CERN and at our institutions worldwide without whom ATLAS could not be operated efficiently.

The crucial computing support from all WLCG partners is acknowledged gratefully, in particular from CERN, the ATLAS Tier-1 facilities at TRIUMF/SFU (Canada), NDGF (Denmark, Norway, Sweden), CC-IN2P3 (France), KIT/GridKA (Germany), INFN-CNAF

JHEP01(2025)053

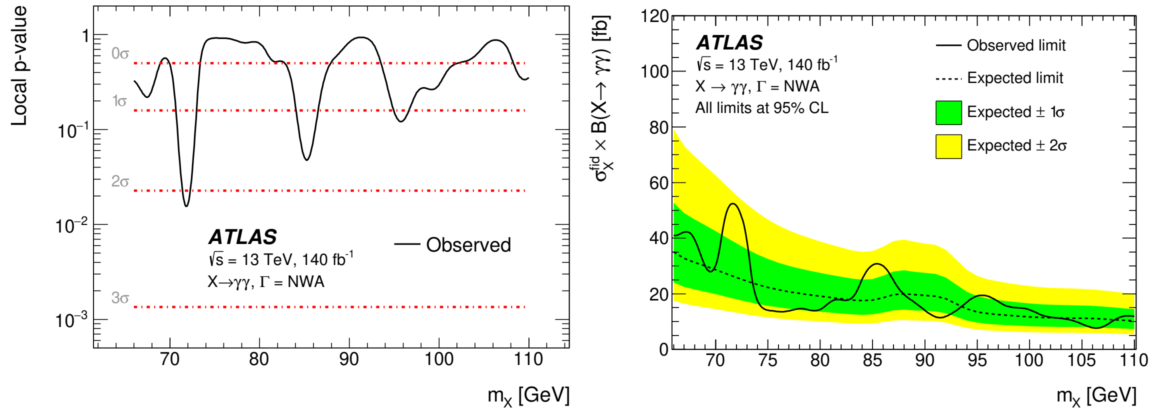

(a) (b)

Figure 6. (a) Compatibility of the data, in the model-independent search, in terms of local p-value (solid line), with the background-only hypothesis as a function of the assumed NWA signal mass m_X. The dotted-dashed lines correspond to the standard deviation quantification σ. (b) 95% CL upper limits on the fiducial cross-section times branching ratio $\mathcal{B}(X \to \gamma\gamma)$ as a function of NWA m_X, where the solid (dashed) line corresponds to the observed (expected) limit and the green (yellow) band corresponds to one (two) standard deviation from the expectation.

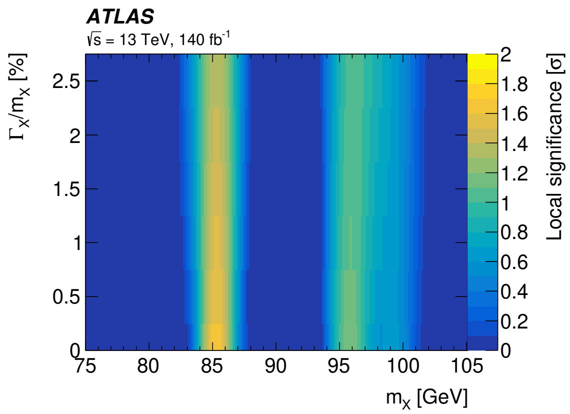

Figure 7. Compatibility of the data with the background-only hypothesis, using the local p_0 quantified in units of standard deviations, σ, as a function of the assumed signal mass m_{X} and of the relative width $\Gamma_{\mathrm{X}}/m_{\mathrm{X}}$ for the model-independent search.

(Italy), NL-T1 (Netherlands), PIC (Spain), RAL (UK) and BNL (USA), the Tier-2 facilities worldwide and large non-WLCG resource providers. Major contributors of computing resources are listed in ref. [63].

We gratefully acknowledge the support of ANPCyT, Argentina; YerPhI, Armenia; ARC, Australia; BMWFW and FWF, Austria; ANAS, Azerbaijan; CNPq and FAPESP, Brazil; NSERC, NRC and CFI, Canada; CERN; ANID, Chile; CAS, MOST and NSFC, China; Minciencias, Colombia; MEYS CR, Czech Republic; DNRF and DNSRC, Denmark; IN2P3-CNRS and CEA-DRF/IRFU, France; SRNSFG, Georgia; BMBF, HGF and MPG, Germany; GSRI, Greece; RGC and Hong Kong SAR, China; ISF and Benoziyo Center, Israel; INFN, Italy; MEXT and JSPS, Japan; CNRST, Morocco; NWO, Netherlands; RCN, Norway;

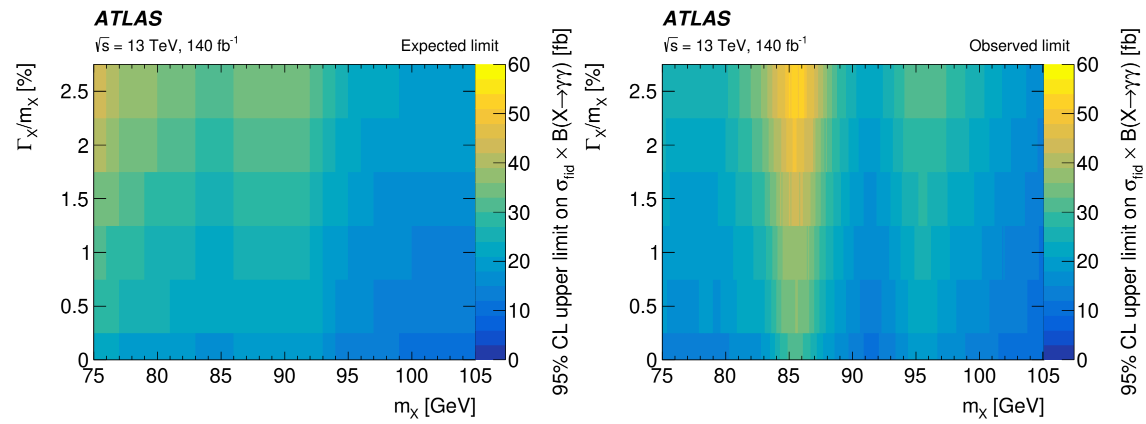

(a) (b)

Figure 8. (a) Expected and (b) observed limits on the fiducial cross-section times branching ratio $\mathcal{B}(X \rightarrow \gamma\gamma)$ computed using the asymptotic approximation as a function of the assumed signal mass m_{X} and relative width $\Gamma_{\mathrm{X}}/m_{\mathrm{X}}$ for the model-independent scalar resonance search.

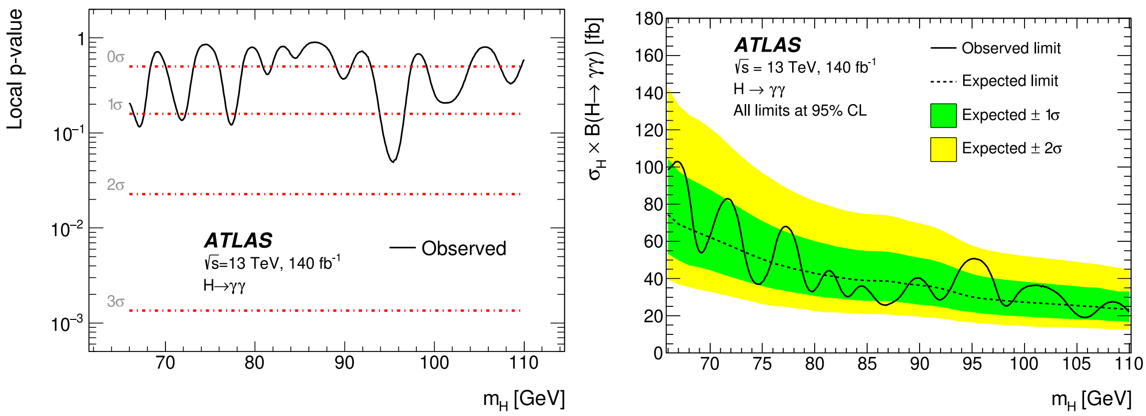

(a) (b)

Figure 9. (a) Compatibility of the data with the background-only hypothesis as quantified by the local p-value (solid line) as a function of the assumed signal mass m_H, for the model-dependent search. The dotted-dashed lines correspond to the standard deviation quantification σ. (b) 95% CL upper limits on the total cross-section times branching ratio $\mathcal{B}(H \rightarrow \gamma\gamma)$ as a function of m_H, where the solid (dashed) line corresponds to the observed (expected) limit and the green (yellow) band corresponds to one (two) standard deviation from the expectation.

MEiN, Poland; FCT, Portugal; MNE/IFA, Romania; MESTD, Serbia; MSSR, Slovakia; ARIS and MVZI, Slovenia; DSI/NRF, South Africa; MICINN, Spain; SRC and Wallenberg Foundation, Sweden; SERI, SNSF and Cantons of Bern and Geneva, Switzerland; NSTC, Taipei; TENMAK, Türkiye; STFC/UKRI, United Kingdom; DOE and NSF, United States of America.

Individual groups and members have received support from BCKDF, CANARIE, CRC and DRAC, Canada; CERN-CZ, PRIMUS 21/SCI/017 and UNCE SCI/013, Czech Republic; COST, ERC, ERDF, Horizon 2020, ICSC-NextGenerationEU and Marie Skłodowska-Curie Actions, European Union; Investissements d'Avenir Labex, Investissements d'Avenir Idex

JHEP01(2025)053

and ANR, France; DFG and AvH Foundation, Germany; Herakleitos, Thales and Aristeia programmes co-financed by EU-ESF and the Greek NSRF, Greece; BSF-NSF and MINERVA, Israel; Norwegian Financial Mechanism 2014-2021, Norway; NCN and NAWA, Poland; La Caixa Banking Foundation, CERCA Programme Generalitat de Catalunya and PROMETEO and GenT Programmes Generalitat Valenciana, Spain; Göran Gustafssons Stiftelse, Sweden; The Royal Society and Leverhulme Trust, United Kingdom.

In addition, individual members wish to acknowledge support from CERN: European Organization for Nuclear Research (CERN PJAS); Chile: Agencia Nacional de Investigación y Desarrollo (FONDECYT 1190886, FONDECYT 1210400, FONDECYT 1230812, FONDECYT 1230987); China: National Natural Science Foundation of China (NSFC - 12175119, NSFC 12275265, NSFC-12075060); Czech Republic: PRIMUS Research Programme (PRIMUS/21/SCI/017); EU: H2020 European Research Council (ERC - 101002463); European Union: European Research Council (ERC - 948254), Horizon 2020 Framework Programme (MUCCA - CHIST-ERA-19-XAI-00), European Union, Future Artificial Intelligence Research (FAIR-NextGenerationEU PE00000013), Italian Center for High Performance Computing, Big Data and Quantum Computing (ICSC, NextGenerationEU), Marie Sklodowska-Curie Actions (EU H2020 MSC IF GRANT NO 101033496); France: Agence Nationale de la Recherche (ANR-20-CE31-0013, ANR-21-CE31-0013, ANR-21-CE31-0022, ANR-22-EDIR-0002), Investissements d'Avenir Idex (ANR-11-LABX-0012), Investissements d'Avenir Labex (ANR-11-LABX-0012); Germany: Baden-Württemberg Stiftung (BW Stiftung-Postdoc Eliteprogramme), Deutsche Forschungsgemeinschaft (DFG - 469666862, DFG - CR 312/5-1); Italy: Istituto Nazionale di Fisica Nucleare (FELLINI G.A. n. 754496, ICSC, NextGenerationEU); Japan: Japan Society for the Promotion of Science (JSPS KAKENHI JP21H05085, JSPS KAKENHI JP22H01227, JSPS KAKENHI JP22H04944, JSPS KAKENHI JP22KK0227); Netherlands: Netherlands Organisation for Scientific Research (NWO Veni 2020 - VI.Veni.202.179); Norway: Research Council of Norway (RCN-314472); Poland: Polish National Agency for Academic Exchange (PPN/PPO/2020/1/00002/U/00001), Polish National Science Centre (NCN 2021/42/E/ST2/00350, NCN OPUS nr 2022/47/B/ST2/03059, NCN UMO-2019/34/E/ST2/00393, UMO-2020/37/B/ST2/01043, UMO-2021/40/C/ST2/00187); Slovenia: Slovenian Research Agency (ARIS grant J1-3010); Spain: BBVA Foundation (LEO22-1-603), Generalitat Valenciana (Artemisa, FEDER, IDIFEDER/2018/048), La Caixa Banking Foundation (LCF/BQ/PI20/11760025), Ministry of Science and Innovation (MCIN & NextGenEU PCI2022-135018-2, MICIN & FEDER PID2021-125273NB, RYC2019-028510-I, RYC2020-030254-I, RYC2021-031273-I, RYC2022-038164-I), PROMETEO and GenT Programmes Generalitat Valenciana (CIDEGENT/2019/023, CIDEGENT/2019/027); Sweden: Swedish Research Council (VR 2018-00482, VR 2022-03845, VR 2022-04683, VR grant 2021-03651), Knut and Alice Wallenberg Foundation (KAW 2017.0100, KAW 2018.0157, KAW 2018.0458, KAW 2019.0447); Switzerland: Swiss National Science Foundation (SNSF - PCEFP2_194658); United Kingdom: Leverhulme Trust (Leverhulme Trust RPG-2020-004); United States of America: U.S. Department of Energy (ECA DE-AC02-76SF00515), Neubauer Family Foundation.

Data Availability Statement. This article has no associated data or the data will not be deposited.

Code Availability Statement. This article has no associated code or the code will not be deposited.

References

[1] A. Celis, V. Ilisie and A. Pich, *LHC constraints on two-Higgs doublet models*, *JHEP* **07** (2013) 053 [arXiv:1302.4022] [INSPIRE].

[2] P.J. Fox and N. Weiner, *Light Signals from a Lighter Higgs*, *JHEP* **08** (2018) 025 [arXiv:1710.07649] [INSPIRE].

[3] T. Biekötter, M. Chakraborti and S. Heinemeyer, *A 96 GeV Higgs boson in the N2HDM*, *Eur. Phys. J. C* **80** (2020) 2 [arXiv:1903.11661] [INSPIRE].

[4] M. Maniatis, *The Next-to-Minimal Supersymmetric extension of the Standard Model reviewed*, *Int. J. Mod. Phys. A* **25** (2010) 3505 [arXiv:0906.0777] [INSPIRE].

[5] B. Bellazzini et al., *R-axion at colliders*, *Phys. Rev. Lett.* **119** (2017) 141804 [arXiv:1702.02152] [INSPIRE].

[6] J.M. Cline and T. Toma, *Pseudo-Goldstone dark matter confronts cosmic ray and collider anomalies*, *Phys. Rev. D* **100** (2019) 035023 [arXiv:1906.02175] [INSPIRE].

[7] K.S. Jeong, T.H. Jung and C.S. Shin, *Axionic Electroweak Baryogenesis*, *Phys. Lett. B* **790** (2019) 326 [arXiv:1806.02591] [INSPIRE].

[8] LHC Higgs Cross Section Working Group collaboration, *Handbook of LHC Higgs Cross Sections: 3. Higgs Properties*, arXiv:1307.1347 [DOI:10.5170/CERN-2013-004] [INSPIRE].

[9] C.E. Rasmussen and C.K.I. Williams, *Gaussian Processes for Machine Learning*, MIT Press (2006).

[10] ATLAS collaboration, *Search for Scalar Diphoton Resonances in the Mass Range* $65-600$ *GeV with the ATLAS Detector in pp Collision Data at* $\sqrt{s}=8$ *TeV*, *Phys. Rev. Lett.* **113** (2014) 171801 [arXiv:1407.6583] [INSPIRE].

[11] CMS collaboration, *Search for a standard model-like Higgs boson in the mass range between 70 and 110 GeV in the diphoton final state in proton-proton collisions at* $\sqrt{s}=8$ *and 13 TeV*, *Phys. Lett. B* **793** (2019) 320 [arXiv:1811.08459] [INSPIRE].

[12] CMS collaboration, *Search for a standard model-like Higgs boson in the mass range between 70 and 110 GeV in the diphoton final state in proton-proton collisions at* $\sqrt{s}=13$ *TeV*, arXiv:2405.18149 [INSPIRE].

[13] ATLAS collaboration, *The ATLAS Experiment at the CERN Large Hadron Collider*, 2008 *JINST* **3** S08003 [INSPIRE].

[14] G. Avoni et al., *The new LUCID-2 detector for luminosity measurement and monitoring in ATLAS*, 2018 *JINST* **13** P07017 [INSPIRE].

[15] ATLAS collaboration, *Performance of the ATLAS Trigger System in 2015*, *Eur. Phys. J. C* **77** (2017) 317 [arXiv:1611.09661] [INSPIRE].

JHEP01(2025)053

[16] ATLAS collaboration, *Software and computing for Run 3 of the ATLAS experiment at the LHC*, arXiv:2404.06335 [INSPIRE].

[17] ATLAS collaboration, *Luminosity determination in pp collisions at $\sqrt{s} = 13$ TeV using the ATLAS detector at the LHC*, Eur. Phys. J. C **83** (2023) 982 [arXiv:2212.09379] [INSPIRE].

[18] ATLAS collaboration, *ATLAS data quality operations and performance for 2015–2018 data-taking*, 2020 *JINST* **15** P04003 [arXiv:1911.04632] [INSPIRE].

[19] ATLAS collaboration, *Electron and photon efficiencies in LHC Run 2 with the ATLAS experiment*, JHEP **05** (2024) 162 [arXiv:2308.13362] [INSPIRE].

[20] ATLAS collaboration, *Performance of electron and photon triggers in ATLAS during LHC Run 2*, Eur. Phys. J. C **80** (2020) 47 [arXiv:1909.00761] [INSPIRE].

[21] ATLAS collaboration, *Estimate of the m_H shift due to interference between signal and background processes in the $H \to \gamma\gamma$ channel, for the $\sqrt{s} = 8$ TeV dataset recorded by ATLAS*, ATL-PHYS-PUB-2016-009, CERN, Geneva (2016).

[22] T. Gleisberg et al., *Event generation with SHERPA 1.1*, JHEP **02** (2009) 007 [arXiv:0811.4622] [INSPIRE].

[23] SHERPA collaboration, *Event Generation with Sherpa 2.2*, SciPost Phys. **7** (2019) 034 [arXiv:1905.09127] [INSPIRE].

[24] F. Siegert, *A practical guide to event generation for prompt photon production with Sherpa*, J. Phys. G **44** (2017) 044007 [arXiv:1611.07226] [INSPIRE].

[25] S. Schumann and F. Krauss, *A parton shower algorithm based on Catani-Seymour dipole factorisation*, JHEP **03** (2008) 038 [arXiv:0709.1027] [INSPIRE].

[26] S. Hoeche, F. Krauss, M. Schonherr and F. Siegert, *QCD matrix elements + parton showers: The NLO case*, JHEP **04** (2013) 027 [arXiv:1207.5030] [INSPIRE].

[27] H.-L. Lai et al., *New parton distributions for collider physics*, Phys. Rev. D **82** (2010) 074024 [arXiv:1007.2241] [INSPIRE].

[28] S. Alioli, P. Nason, C. Oleari and E. Re, *A general framework for implementing NLO calculations in shower Monte Carlo programs: the POWHEG BOX*, JHEP **06** (2010) 043 [arXiv:1002.2581] [INSPIRE].

[29] S. Alioli, P. Nason, C. Oleari and E. Re, *NLO vector-boson production matched with shower in POWHEG*, JHEP **07** (2008) 060 [arXiv:0805.4802] [INSPIRE].

[30] T. Sjostrand, S. Mrenna and P.Z. Skands, *A Brief Introduction to PYTHIA 8.1*, Comput. Phys. Commun. **178** (2008) 852 [arXiv:0710.3820] [INSPIRE].

[31] ATLAS collaboration, *Measurement of the Z/γ^* boson transverse momentum distribution in pp collisions at $\sqrt{s} = 7$ TeV with the ATLAS detector*, JHEP **09** (2014) 145 [arXiv:1406.3660] [INSPIRE].

[32] J. Pumplin et al., *New generation of parton distributions with uncertainties from global QCD analysis*, JHEP **07** (2002) 012 [hep-ph/0201195] [INSPIRE].

[33] ATLAS collaboration, *ATLAS Pythia 8 tunes to 7 TeV data*, ATL-PHYS-PUB-2014-021, CERN, Geneva (2014).

[34] ATLAS collaboration, *Summary of ATLAS Pythia 8 tunes*, ATL-PHYS-PUB-2012-003, CERN, Geneva (2012).

JHEP01(2025)053

[35] A.D. Martin, W.J. Stirling, R.S. Thorne and G. Watt, *Parton distributions for the LHC*, *Eur. Phys. J. C* **63** (2009) 189 [arXiv:0901.0002] [INSPIRE].

[36] ATLAS collaboration, *The ATLAS Simulation Infrastructure*, *Eur. Phys. J. C* **70** (2010) 823 [arXiv:1005.4568] [INSPIRE].

[37] GEANT4 collaboration, *GEANT4 — a simulation toolkit*, *Nucl. Instrum. Meth. A* **506** (2003) 250 [INSPIRE].

[38] ATLAS collaboration, *The simulation principle and performance of the ATLAS fast calorimeter simulation FastCaloSim*, ATL-PHYS-PUB-2010-013, CERN, Geneva (2010).

[39] ATLAS collaboration, *Measurements of the Higgs boson inclusive and differential fiducial cross-sections in the diphoton decay channel with pp collisions at $\sqrt{s} = 13$ TeV with the ATLAS detector*, *JHEP* **08** (2022) 027 [arXiv:2202.00487] [INSPIRE].

[40] ATLAS collaboration, *Electron and photon performance measurements with the ATLAS detector using the 2015–2017 LHC proton-proton collision data*, 2019 *JINST* **14** P12006 [arXiv:1908.00005] [INSPIRE].

[41] ATLAS collaboration, *Measurement of the photon identification efficiencies with the ATLAS detector using LHC Run 2 data collected in 2015 and 2016*, *Eur. Phys. J. C* **79** (2019) 205 [arXiv:1810.05087] [INSPIRE].

[42] ATLAS collaboration, *Electron and photon energy calibration with the ATLAS detector using LHC Run 2 data*, 2024 *JINST* **19** P02009 [arXiv:2309.05471] [INSPIRE].

[43] ATLAS collaboration, *Vertex Reconstruction Performance of the ATLAS Detector at $\sqrt{s} = 13$ TeV*, ATL-PHYS-PUB-2015-026, CERN, Geneva (2015).

[44] ATLAS collaboration, *Measurement of Higgs boson production in the diphoton decay channel in pp collisions at center-of-mass energies of 7 and 8 TeV with the ATLAS detector*, *Phys. Rev. D* **90** (2014) 112015 [arXiv:1408.7084] [INSPIRE].

[45] ATLAS collaboration, *Topological cell clustering in the ATLAS calorimeters and its performance in LHC Run 1*, *Eur. Phys. J. C* **77** (2017) 490 [arXiv:1603.02934] [INSPIRE].

[46] ATLAS collaboration, *Measurement of the inclusive isolated prompt photon cross section in pp collisions at $\sqrt{s} = 7$ TeV with the ATLAS detector*, *Phys. Rev. D* **83** (2011) 052005 [arXiv:1012.4389] [INSPIRE].

[47] M. Cacciari, G.P. Salam and G. Soyez, *The Catchment Area of Jets*, *JHEP* **04** (2008) 005 [arXiv:0802.1188] [INSPIRE].

[48] M. Cacciari, G.P. Salam and S. Sapeta, *On the characterisation of the underlying event*, *JHEP* **04** (2010) 065 [arXiv:0912.4926] [INSPIRE].

[49] G. Ke et al., *LightGBM: a highly efficient gradient boosting decision tree*, in I. Guyon et al. eds., *Advances in Neural Information Processing Systems*, Curran Associates, Inc. 2017, https://proceedings.neurips.cc/paper_files/paper/2017/file/6449f44a102fde848669bdd9eb6b76fa-Paper.pdf.

[50] Y. Freund and R.E. Schapire, *A Decision-Theoretic Generalization of On-Line Learning and an Application to Boosting*, *J. Comput. Syst. Sci.* **55** (1997) 119 [INSPIRE].

[51] A. Hoecker et al., *TMVA - Toolkit for Multivariate Data Analysis*, physics/0703039.

[52] M. Oreglia, *A Study of the Reactions $\psi' \to \gamma\gamma\psi$*, Ph.D. thesis, SLAC (1980).

[53] ATLAS collaboration, *Search for resonances in diphoton events at $\sqrt{s} = 13$ TeV with the ATLAS detector*, *JHEP* **09** (2016) 001 [arXiv:1606.03833] [INSPIRE].

JHEP01(2025)053

[54] LHC Higgs Cross Section Working Group collaboration, *Handbook of LHC Higgs Cross Sections: 4. Deciphering the Nature of the Higgs Sector*, arXiv:1610.07922 [DOI:10.23731/CYRM-2017-002] [INSPIRE].

[55] ATLAS collaboration, *Measurement of isolated-photon pair production in pp collisions at $\sqrt{s} = 7$ TeV with the ATLAS detector*, JHEP **01** (2013) 086 [arXiv:1211.1913] [INSPIRE].

[56] ATLAS collaboration, *Measurements of Higgs boson properties in the diphoton decay channel with 36 fb^{-1} of pp collision data at $\sqrt{s} = 13$ TeV with the ATLAS detector*, Phys. Rev. D **98** (2018) 052005 [arXiv:1802.04146] [INSPIRE].

[57] ATLAS collaboration, *Search for boosted diphoton resonances in the 10 to 70 GeV mass range using 138 fb^{-1} of 13 TeV pp collisions with the ATLAS detector*, JHEP **07** (2023) 155 [arXiv:2211.04172] [INSPIRE].

[58] M.N. Gibbs, *Bayesian Gaussian Processes for Regression and Classification*, Ph.D. thesis, University of Cambridge, U.K. (1997).

[59] S. Bernstein, *Démonstration du Théorème de Weierstrass fondée sur le calcul des Probabilités*, *Comm. Soc. Math. Kharkov* **13** (1912) 1.

[60] L. Devroye, *Sample-based non-uniform random variate generation*, in the proceedings of the *18th conference on Winter simulation - WSC '86*, Washington D.C., U.S.A., 8–10 December (1986) [DOI:10.1145/318242.318443].

[61] G. Cowan, K. Cranmer, E. Gross and O. Vitells, *Asymptotic formulae for likelihood-based tests of new physics*, Eur. Phys. J. C **71** (2011) 1554 [*Erratum ibid.* **73** (2013) 2501] [arXiv:1007.1727] [INSPIRE].

[62] A.L. Read, *Presentation of search results: The CL_s technique*, J. Phys. G **28** (2002) 2693 [INSPIRE].

[63] ATLAS collaboration, *ATLAS Computing Acknowledgements*, ATL-SOFT-PUB-2023-001, CERN, Geneva (2023).

JHEP01(2025)053

The ATLAS collaboration

G. Aad[102], B. Abbott[120], K. Abeling[55], N.J. Abicht[49], S.H. Abidi[29], A. Aboulhorma[35e], H. Abramowicz[152], H. Abreu[151], Y. Abulaiti[117], B.S. Acharya[69a,69b,m], C. Adam Bourdarios[4], L. Adamczyk[86a], S.V. Addepalli[26], M.J. Addison[101], J. Adelman[115], A. Adiguzel[21c], T. Adye[134], A.A. Affolder[136], Y. Afik[39], M.N. Agaras[13], J. Agarwala[73a,73b], A. Aggarwal[100], C. Agheorghiesei[27c], A. Ahmad[36], F. Ahmadov[38,aa], W.S. Ahmed[104], S. Ahuja[95], X. Ai[62e], G. Aielli[76a,76b], A. Aikot[163], M. Ait Tamlihat[35e], B. Aitbenchikh[35a], I. Aizenberg[169], M. Akbiyik[100], T.P.A. Åkesson[98], A.V. Akimov[37], D. Akiyama[168], N.N. Akolkar[24], S. Aktas[21a], K. Al Khoury[41], G.L. Alberghi[23b], J. Albert[165], P. Albicocco[53], G.L. Albouy[60], S. Alderweireldt[52], Z.L. Alegria[121], M. Aleksa[36], I.N. Aleksandrov[38], C. Alexa[27b], T. Alexopoulos[10], F. Alfonsi[23b], M. Algren[56], M. Alhroob[120], B. Ali[132], H.M.J. Ali[91], S. Ali[149], S.W. Alibocus[92], M. Aliev[33c], G. Alimonti[71a], W. Alkakhi[55], C. Allaire[66], B.M.M. Allbrooke[147], J.F. Allen[52], C.A. Allendes Flores[137f], P.P. Allport[20], A. Aloisio[72a,72b], F. Alonso[90], C. Alpigiani[139], M. Alvarez Estevez[99], A. Alvarez Fernandez[100], M. Alves Cardoso[56], M.G. Alviggi[72a,72b], M. Aly[101], Y. Amaral Coutinho[83b], A. Ambler[104], C. Amelung[36], M. Amerl[101], C.G. Ames[109], D. Amidei[106], S.P. Amor Dos Santos[130a], K.R. Amos[163], V. Ananiev[125], C. Anastopoulos[140], T. Andeen[11], J.K. Anders[36], S.Y. Andrean[47a,47b], A. Andreazza[71a,71b], S. Angelidakis[9], A. Angerami[41,ad], A.V. Anisenkov[37], A. Annovi[74a], C. Antel[56], M.T. Anthony[140], E. Antipov[146], M. Antonelli[53], F. Anulli[75a], M. Aoki[84], T. Aoki[154], J.A. Aparisi Pozo[163], M.A. Aparo[147], L. Aperio Bella[48], C. Appelt[18], A. Apyan[26], N. Aranzabal[36], S.J. Arbiol Val[87], C. Arcangeletti[53], A.T.H. Arce[51], E. Arena[92], J-F. Arguin[108], S. Argyropoulos[54], J.-H. Arling[48], O. Arnaez[4], H. Arnold[114], G. Artoni[75a,75b], H. Asada[111], K. Asai[118], S. Asai[154], N.A. Asbah[61], J. Assahsah[35d], K. Assamagan[29], R. Astalos[28a], S. Atashi[159], R.J. Atkin[33a], M. Atkinson[162], H. Atmani[35f], P.A. Atmasiddha[128], K. Augsten[132], S. Auricchio[72a,72b], A.D. Auriol[20], V.A. Austrup[101], G. Avolio[36], K. Axiotis[56], G. Azuelos[108,ah], D. Babal[28b], H. Bachacou[135], K. Bachas[153,q], A. Bachiu[34], F. Backman[47a,47b], A. Badea[61], T.M. Baer[106], P. Bagnaia[75a,75b], M. Bahmani[18], D. Bahner[54], A.J. Bailey[163], V.R. Bailey[162], J.T. Baines[134], L. Baines[94], O.K. Baker[172], E. Bakos[15], D. Bakshi Gupta[8], V. Balakrishnan[120], R. Balasubramanian[114], E.M. Baldin[37], P. Balek[86a], E. Ballabene[23b,23a], F. Balli[135], L.M. Baltes[63a], W.K. Balunas[32], J. Balz[100], E. Banas[87], M. Bandieramonte[129], A. Bandyopadhyay[24], S. Bansal[24], L. Barak[152], M. Barakat[48], E.L. Barberio[105], D. Barberis[57b,57a], M. Barbero[102], M.Z. Barel[114], K.N. Barends[33a], T. Barillari[110], M-S. Barisits[36], T. Barklow[144], P. Baron[122], D.A. Baron Moreno[101], A. Baroncelli[62a], G. Barone[29], A.J. Barr[126], J.D. Barr[96], L. Barranco Navarro[47a,47b], F. Barreiro[99], J. Barreiro Guimarães da Costa[14a], U. Barron[152], M.G. Barros Teixeira[130a], S. Barsov[37], F. Bartels[63a], R. Bartoldus[144], A.E. Barton[91], P. Bartos[28a], A. Basan[100], M. Baselga[49], A. Bassalat[66,b], M.J. Basso[156a], C.R. Basson[101], R.L. Bates[59], S. Batlamous[35e], J.R. Batley[32], B. Batool[142], M. Battaglia[136], D. Battulga[18], M. Bauce[75a,75b], M. Bauer[36], P. Bauer[24], L.T. Bazzano Hurrell[30], J.B. Beacham[51], T. Beau[127], J.Y. Beaucamp[90], P.H. Beauchemin[158], P. Bechtle[24], H.P. Beck[19,p], K. Becker[167], A.J. Beddall[82], V.A. Bednyakov[38], C.P. Bee[146], L.J. Beemster[15], T.A. Beermann[36], M. Begalli[83d], M. Begel[29], A. Behera[146], J.K. Behr[48], J.F. Beirer[36],

JHEP01(2025)053

F. Beisiegel[24], M. Belfkir[116b], G. Bella[152], L. Bellagamba[23b], A. Bellerive[34], P. Bellos[20], K. Beloborodov[37], D. Benchekroun[35a], F. Bendebba[35a], Y. Benhammou[152], M. Benoit[29], S. Bentvelsen[114], L. Beresford[48], M. Beretta[53], E. Bergeaas Kuutmann[161], N. Berger[4], B. Bergmann[132], J. Beringer[17a], G. Bernardi[5], C. Bernius[144], F.U. Bernlochner[24], F. Bernon[36,102], A. Berrocal Guardia[13], T. Berry[95], P. Berta[133], A. Berthold[50], I.A. Bertram[91], S. Bethke[110], A. Betti[75a,75b], A.J. Bevan[94], N.K. Bhalla[54], M. Bhamjee[33c], S. Bhatta[146], D.S. Bhattacharya[166], P. Bhattarai[144], K.D. Bhide[54], V.S. Bhopatkar[121], R.M. Bianchi[129], G. Bianco[23b,23a], O. Biebel[109], R. Bielski[123], M. Biglietti[77a], M. Bindi[55], A. Bingul[21b], C. Bini[75a,75b], A. Biondini[92], C.J. Birch-sykes[101], G.A. Bird[32,134], M. Birman[169], M. Biros[133], S. Biryukov[147], T. Bisanz[49], E. Bisceglie[43b,43a], J.P. Biswal[134], D. Biswas[142], A. Bitadze[101], K. Bjørke[125], I. Bloch[48], A. Blue[59], U. Blumenschein[94], J. Blumenthal[100], G.J. Bobbink[114], V.S. Bobrovnikov[37], M. Boehler[54], B. Boehm[166], D. Bogavac[36], A.G. Bogdanchikov[37], C. Bohm[47a], V. Boisvert[95], P. Bokan[36], T. Bold[86a], M. Bomben[5], M. Bona[94], M. Boonekamp[135], C.D. Booth[95], A.G. Borbély[59], I.S. Bordulev[37], H.M. Borecka-Bielska[108], G. Borissov[91], D. Bortoletto[126], D. Boscherini[23b], M. Bosman[13], J.D. Bossio Sola[36], K. Bouaouda[35a], N. Bouchhar[163], J. Boudreau[129], E.V. Bouhova-Thacker[91], D. Boumediene[40], R. Bouquet[165], A. Boveia[119], J. Boyd[36], D. Boye[29], I.R. Boyko[38], J. Bracinik[20], N. Brahimi[62d], G. Brandt[171], O. Brandt[32], F. Braren[48], B. Brau[103], J.E. Brau[123], R. Brener[169], L. Brenner[114], R. Brenner[161], S. Bressler[169], D. Britton[59], D. Britzger[110], I. Brock[24], R. Brock[107], G. Brooijmans[41], W.K. Brooks[137f], E. Brost[29], L.M. Brown[165], L.E. Bruce[61], T.L. Bruckler[126], P.A. Bruckman de Renstrom[87], B. Brüers[48], A. Bruni[23b], G. Bruni[23b], M. Bruschi[23b], N. Bruscino[75a,75b], T. Buanes[16], Q. Buat[139], D. Buchin[110], A.G. Buckley[59], O. Bulekov[37], B.A. Bullard[144], S. Burdin[92], C.D. Burgard[49], A.M. Burger[40], B. Burghgrave[8], O. Burlayenko[54], J.T.P. Burr[32], C.D. Burton[11], J.C. Burzynski[143], E.L. Busch[41], V. Büscher[100], P.J. Bussey[59], J.M. Butler[25], C.M. Buttar[59], J.M. Butterworth[96], W. Buttinger[134], C.J. Buxo Vazquez[107], A.R. Buzykaev[37], S. Cabrera Urbán[163], L. Cadamuro[66], D. Caforio[58], H. Cai[129], Y. Cai[14a,14e], Y. Cai[14c], V.M.M. Cairo[36], O. Cakir[3a], N. Calace[36], P. Calafiura[17a], G. Calderini[127], P. Calfayan[68], G. Callea[59], L.P. Caloba[83b], D. Calvet[40], S. Calvet[40], M. Calvetti[74a,74b], R. Camacho Toro[127], S. Camarda[36], D. Camarero Munoz[26], P. Camarri[76a,76b], M.T. Camerlingo[72a,72b], D. Cameron[36], C. Camincher[165], M. Campanelli[96], A. Camplani[42], V. Canale[72a,72b], A. Canesse[104], J. Cantero[163], Y. Cao[162], F. Capocasa[26], M. Capua[43b,43a], A. Carbone[71a,71b], R. Cardarelli[76a], J.C.J. Cardenas[8], F. Cardillo[163], G. Carducci[43b,43a], T. Carli[36], G. Carlino[72a], J.I. Carlotto[13], B.T. Carlson[129,r], E.M. Carlson[165,156a], L. Carminati[71a,71b], A. Carnelli[135], M. Carnesale[75a,75b], S. Caron[113], E. Carquin[137f], S. Carrá[71a], G. Carratta[23b,23a], J.W.S. Carter[155], T.M. Carter[52], M.P. Casado[13,i], M. Caspar[48], F.L. Castillo[4], L. Castillo Garcia[13], V. Castillo Gimenez[163], N.F. Castro[130a,130e], A. Catinaccio[36], J.R. Catmore[125], T. Cavaliere[4], V. Cavaliere[29], N. Cavalli[23b,23a], V. Cavasinni[74a,74b], Y.C. Cekmecelioglu[48], E. Celebi[21a], F. Celli[126], M.S. Centonze[70a,70b], V. Cepaitis[56], K. Cerny[122], A.S. Cerqueira[83a], A. Cerri[147], L. Cerrito[76a,76b], F. Cerutti[17a],

B. Cervato[142], A. Cervelli[23b], G. Cesarini[53], S.A. Cetin[82], D. Chakraborty[115], J. Chan[17a], W.Y. Chan[154], J.D. Chapman[32], E. Chapon[135], B. Chargeishvili[150b], D.G. Charlton[20], M. Chatterjee[19], C. Chauhan[133], Y. Che[14c], S. Chekanov[6], S.V. Chekulaev[156a], G.A. Chelkov[38,a], A. Chen[106], B. Chen[152], B. Chen[165], H. Chen[14c], H. Chen[29], J. Chen[62c], J. Chen[143], M. Chen[126], S. Chen[154], S.J. Chen[14c], X. Chen[62c,135], X. Chen[14b,ag], Y. Chen[62a], C.L. Cheng[170], H.C. Cheng[64a], S. Cheong[144], A. Cheplakov[38], E. Cheremushkina[48], E. Cherepanova[114], R. Cherkaoui El Moursli[35e], E. Cheu[7], K. Cheung[65], L. Chevalier[135], V. Chiarella[53], G. Chiarelli[74a], N. Chiedde[102], G. Chiodini[70a], A.S. Chisholm[20], A. Chitan[27b], M. Chitishvili[163], M.V. Chizhov[38,s], K. Choi[11], A.R. Chomont[75a,75b], Y. Chou[139], E.Y.S. Chow[113], T. Chowdhury[33g], K.L. Chu[169], M.C. Chu[64a], X. Chu[14a,14e], J. Chudoba[131], J.J. Chwastowski[87], D. Cieri[110], K.M. Ciesla[86a], V. Cindro[93], A. Ciocio[17a], F. Cirotto[72a,72b], Z.H. Citron[169,k], M. Citterio[71a], D.A. Ciubotaru[27b], A. Clark[56], P.J. Clark[52], C. Clarry[155], J.M. Clavijo Columbie[48], S.E. Clawson[48], C. Clement[47a,47b], J. Clercx[48], Y. Coadou[102], M. Cobal[69a,69c], A. Coccaro[57b], R.F. Coelho Barrue[130a], R. Coelho Lopes De Sa[103], S. Coelli[71a], B. Cole[41], J. Collot[60], P. Conde Muiño[130a,130g], M.P. Connell[33c], S.H. Connell[33c], I.A. Connelly[59], E.I. Conroy[126], F. Conventi[72a,ai], H.G. Cooke[20], A.M. Cooper-Sarkar[126], A. Cordeiro Oudot Choi[127], L.D. Corpe[40], M. Corradi[75a,75b], F. Corriveau[104,y], A. Cortes-Gonzalez[18], M.J. Costa[163], F. Costanza[4], D. Costanzo[140], B.M. Cote[119], G. Cowan[95], K. Cranmer[170], D. Cremonini[23b,23a], S. Crépé-Renaudin[60], F. Crescioli[127], M. Cristinziani[142], M. Cristoforetti[78a,78b], V. Croft[114], J.E. Crosby[121], G. Crosetti[43b,43a], A. Cueto[99], T. Cuhadar Donszelmann[159], H. Cui[14a,14e], Z. Cui[7], W.R. Cunningham[59], F. Curcio[43b,43a], P. Czodrowski[36], M.M. Czurylo[63b], M.J. Da Cunha Sargedas De Sousa[57b,57a], J.V. Da Fonseca Pinto[83b], C. Da Via[101], W. Dabrowski[86a], T. Dado[49], S. Dahbi[33g], T. Dai[106], D. Dal Santo[19], C. Dallapiccola[103], M. Dam[42], G. D'amen[29], V. D'Amico[109], J. Damp[100], J.R. Dandoy[34], M. Danninger[143], V. Dao[36], G. Darbo[57b], S. Darmora[6], S.J. Das[29,ak], S. D'Auria[71a,71b], C. David[33a], T. Davidek[133], B. Davis-Purcell[34], I. Dawson[94], H.A. Day-hall[132], K. De[8], R. De Asmundis[72a], N. De Biase[48], S. De Castro[23b,23a], N. De Groot[113], P. de Jong[114], H. De la Torre[115], A. De Maria[14c], A. De Salvo[75a], U. De Sanctis[76a,76b], F. De Santis[70a,70b], A. De Santo[147], J.B. De Vivie De Regie[60], D.V. Dedovich[38], J. Degens[114], A.M. Deiana[44], F. Del Corso[23b,23a], J. Del Peso[99], F. Del Rio[63a], L. Delagrange[127], F. Deliot[135], C.M. Delitzsch[49], M. Della Pietra[72a,72b], D. Della Volpe[56], A. Dell'Acqua[36], L. Dell'Asta[71a,71b], M. Delmastro[4], P.A. Delsart[60], S. Demers[172], M. Demichev[38], S.P. Denisov[37], L. D'Eramo[40], D. Derendarz[87], F. Derue[127], P. Dervan[92], K. Desch[24], C. Deutsch[24], F.A. Di Bello[57b,57a], A. Di Ciaccio[76a,76b], L. Di Ciaccio[4], A. Di Domenico[75a,75b], C. Di Donato[72a,72b], A. Di Girolamo[36], G. Di Gregorio[36], A. Di Luca[78a,78b], B. Di Micco[77a,77b], R. Di Nardo[77a,77b], M. Diamantopoulou[34], F.A. Dias[114], T. Dias Do Vale[143], M.A. Diaz[137a,137b], F.G. Diaz Capriles[24], M. Didenko[163], E.B. Diehl[106], L. Diehl[54], S. Díez Cornell[48], C. Diez Pardos[142], C. Dimitriadi[161,24], A. Dimitrievska[17a], J. Dingfelder[24], I-M. Dinu[27b], S.J. Dittmeier[63b], F. Dittus[36], F. Djama[102], T. Djobava[150b], C. Doglioni[101,98], A. Dohnalova[28a], J. Dolejsi[133], Z. Dolezal[133], K.M. Dona[39], M. Donadelli[83c],

JHEP01(2025)053

B. Dong[107], J. Donini[40], A. D'Onofrio[72a,72b], M. D'Onofrio[92], J. Dopke[134], A. Doria[72a], N. Dos Santos Fernandes[130a], P. Dougan[101], M.T. Dova[90], A.T. Doyle[59], M.A. Draguet[126], E. Dreyer[169], I. Drivas-koulouris[10], M. Drnevich[117], M. Drozdova[56], D. Du[62a], T.A. du Pree[114], F. Dubinin[37], M. Dubovsky[28a], E. Duchovni[169], G. Duckeck[109], O.A. Ducu[27b], D. Duda[52], A. Dudarev[36], E.R. Duden[26], M. D'uffizi[101], L. Duflot[66], M. Dührssen[36], A.E. Dumitriu[27b], M. Dunford[63a], S. Dungs[49], K. Dunne[47a,47b], A. Duperrin[102], H. Duran Yildiz[3a], M. Düren[58], A. Durglishvili[150b], B.L. Dwyer[115], G.I. Dyckes[17a], M. Dyndal[86a], B.S. Dziedzic[87], Z.O. Earnshaw[147], G.H. Eberwein[126], B. Eckerova[28a], S. Eggebrecht[55], E. Egidio Purcino De Souza[127], L.F. Ehrke[56], G. Eigen[16], K. Einsweiler[17a], T. Ekelof[161], P.A. Ekman[98], S. El Farkh[35b], Y. El Ghazali[35b], H. El Jarrari[36], A. El Moussaouy[108], V. Ellajosyula[161], M. Ellert[161], F. Ellinghaus[171], N. Ellis[36], J. Elmsheuser[29], M. Elsing[36], D. Emeliyanov[134], Y. Enari[154], I. Ene[17a], S. Epari[13], P.A. Erland[87], M. Errenst[171], M. Escalier[66], C. Escobar[163], E. Etzion[152], G. Evans[130a], H. Evans[68], L.S. Evans[95], M.O. Evans[147], A. Ezhilov[37], S. Ezzarqtouni[35a], F. Fabbri[59], L. Fabbri[23b,23a], G. Facini[96], V. Fadeyev[136], R.M. Fakhrutdinov[37], D. Fakoudis[100], S. Falciano[75a], L.F. Falda Ulhoa Coelho[36], P.J. Falke[24], J. Faltova[133], C. Fan[162], Y. Fan[14a], Y. Fang[14a,14e], M. Fanti[71a,71b], M. Faraj[69a,69b], Z. Farazpay[97], A. Farbin[8], A. Farilla[77a], T. Farooque[107], S.M. Farrington[52], F. Fassi[35e], D. Fassouliotis[9], M. Faucci Giannelli[76a,76b], W.J. Fawcett[32], L. Fayard[66], P. Federic[133], P. Federicova[131], O.L. Fedin[37,a], G. Fedotov[37], M. Feickert[170], L. Feligioni[102], D.E. Fellers[123], C. Feng[62b], M. Feng[14b], Z. Feng[114], M.J. Fenton[159], A.B. Fenyuk[37], L. Ferencz[48], R.A.M. Ferguson[91], S.I. Fernandez Luengo[137f], P. Fernandez Martinez[13], M.J.V. Fernoux[102], J. Ferrando[91], A. Ferrari[161], P. Ferrari[114,113], R. Ferrari[73a], D. Ferrere[56], C. Ferretti[106], F. Fiedler[100], P. Fiedler[132], A. Filipčič[93], E.K. Filmer[1], F. Filthaut[113], M.C.N. Fiolhais[130a,130c,c], L. Fiorini[163], W.C. Fisher[107], T. Fitschen[101], P.M. Fitzhugh[135], I. Fleck[142], P. Fleischmann[106], T. Flick[171], M. Flores[33d,ae], L.R. Flores Castillo[64a], L. Flores Sanz De Acedo[36], F.M. Follega[78a,78b], N. Fomin[16], J.H. Foo[155], A. Formica[135], A.C. Forti[101], E. Fortin[36], A.W. Fortman[17a], M.G. Foti[17a], L. Fountas[9,j], D. Fournier[66], H. Fox[91], P. Francavilla[74a,74b], S. Francescato[61], S. Franchellucci[56], M. Franchini[23b,23a], S. Franchino[63a], D. Francis[36], L. Franco[113], V. Franco Lima[36], L. Franconi[48], M. Franklin[61], G. Frattari[26], A.C. Freegard[94], W.S. Freund[83b], Y.Y. Frid[152], J. Friend[59], N. Fritzsche[50], A. Froch[54], D. Froidevaux[36], J.A. Frost[126], Y. Fu[62a], S. Fuenzalida Garrido[137f], M. Fujimoto[102], K.Y. Fung[64a], E. Furtado De Simas Filho[83b], M. Furukawa[154], J. Fuster[163], A. Gabrielli[23b,23a], A. Gabrielli[155], P. Gadow[36], G. Gagliardi[57b,57a], L.G. Gagnon[17a], E.J. Gallas[126], B.J. Gallop[134], K.K. Gan[119], S. Ganguly[154], Y. Gao[52], F.M. Garay Walls[137a,137b], B. Garcia[29], C. García[163], A. Garcia Alonso[114], A.G. Garcia Caffaro[172], J.E. García Navarro[163], M. Garcia-Sciveres[17a], G.L. Gardner[128], R.W. Gardner[39], N. Garelli[158], D. Garg[80], R.B. Garg[144,n], J.M. Gargan[52], C.A. Garner[155], C.M. Garvey[33a], P. Gaspar[83b], V.K. Gassmann[158], G. Gaudio[73a], V. Gautam[13], P. Gauzzi[75a,75b], I.L. Gavrilenko[37], A. Gavrilyuk[37], C. Gay[164], G. Gaycken[48], E.N. Gazis[10], A.A. Geanta[27b], C.M. Gee[136], A. Gekow[119], C. Gemme[57b], M.H. Genest[60], S. Gentile[75a,75b], A.D. Gentry[112], S. George[95], W.F. George[20], T. Geralis[46],

JHEP01(2025)053

P. Gessinger-Befurt[36], M.E. Geyik[171], M. Ghani[167], M. Ghneimat[142], K. Ghorbanian[94], A. Ghosal[142], A. Ghosh[159], A. Ghosh[7], B. Giacobbe[23b], S. Giagu[75a,75b], T. Giani[114], P. Giannetti[74a], A. Giannini[62a], S.M. Gibson[95], M. Gignac[136], D.T. Gil[86b], A.K. Gilbert[86a], B.J. Gilbert[41], D. Gillberg[34], G. Gilles[114], L. Ginabat[127], D.M. Gingrich[2,ah], M.P. Giordani[69a,69c], P.F. Giraud[135], G. Giugliarelli[69a,69c], D. Giugni[71a], F. Giuli[36], I. Gkialas[9,j], L.K. Gladilin[37], C. Glasman[99], G.R. Gledhill[123], G. Glemža[48], M. Glisic[123], I. Gnesi[43b,f], Y. Go[29], M. Goblirsch-Kolb[36], B. Gocke[49], D. Godin[108], B. Gokturk[21a], S. Goldfarb[105], T. Golling[56], M.G.D. Gololo[33g], D. Golubkov[37], J.P. Gombas[107], A. Gomes[130a,130b], G. Gomes Da Silva[142], A.J. Gomez Delegido[163], R. Gonçalo[130a,130c], G. Gonella[123], L. Gonella[20], A. Gongadze[150c], F. Gonnella[20], J.L. Gonski[41], R.Y. González Andana[52], S. González de la Hoz[163], R. Gonzalez Lopez[92], C. Gonzalez Renteria[17a], M.V. Gonzalez Rodrigues[48], R. Gonzalez Suarez[161], S. Gonzalez-Sevilla[56], G.R. Gonzalvo Rodriguez[163], L. Goossens[36], B. Gorini[36], E. Gorini[70a,70b], A. Gorišek[93], T.C. Gosart[128], A.T. Goshaw[51], M.I. Gostkin[38], S. Goswami[121], C.A. Gottardo[36], S.A. Gotz[109], M. Gouighri[35b], V. Goumarre[48], A.G. Goussiou[139], N. Govender[33c], I. Grabowska-Bold[86a], K. Graham[34], E. Gramstad[125], S. Grancagnolo[70a,70b], M. Grandi[147], C.M. Grant[1,135], P.M. Gravila[27f], F.G. Gravili[70a,70b], H.M. Gray[17a], M. Greco[70a,70b], C. Grefe[24], I.M. Gregor[48], P. Grenier[144], S.G. Grewe[110], C. Grieco[13], A.A. Grillo[136], K. Grimm[31], S. Grinstein[13,u], J.-F. Grivaz[66], E. Gross[169], J. Grosse-Knetter[55], C. Grud[106], J.C. Grundy[126], L. Guan[106], W. Guan[29], C. Gubbels[164], J.G.R. Guerrero Rojas[163], G. Guerrieri[69a,69c], F. Guescini[110], R. Gugel[100], J.A.M. Guhit[106], A. Guida[18], E. Guilloton[167,134], S. Guindon[36], F. Guo[14a,14e], J. Guo[62c], L. Guo[48], Y. Guo[106], R. Gupta[48], R. Gupta[129], S. Gurbuz[24], S.S. Gurdasani[54], G. Gustavino[36], M. Guth[56], P. Gutierrez[120], L.F. Gutierrez Zagazeta[128], M. Gutsche[50], C. Gutschow[96], C. Gwenlan[126], C.B. Gwilliam[92], E.S. Haaland[125], A. Haas[117], M. Habedank[48], C. Haber[17a], H.K. Hadavand[8], A. Hadef[50], S. Hadzic[110], A.I. Hagan[91], J.J. Hahn[142], E.H. Haines[96], M. Haleem[166], J. Haley[121], J.J. Hall[140], G.D. Hallewell[102], L. Halser[19], K. Hamano[165], M. Hamer[24], G.N. Hamity[52], E.J. Hampshire[95], J. Han[62b], K. Han[62a], L. Han[14c], L. Han[62a], S. Han[17a], Y.F. Han[155], K. Hanagaki[84], M. Hance[136], D.A. Hangal[41], H. Hanif[143], M.D. Hank[128], J.B. Hansen[42], P.H. Hansen[42], K. Hara[157], D. Harada[56], T. Harenberg[171], S. Harkusha[37], M.L. Harris[103], Y.T. Harris[126], J. Harrison[13], N.M. Harrison[119], P.F. Harrison[167], N.M. Hartman[110], N.M. Hartmann[109], Y. Hasegawa[141], R. Hauser[107], C.M. Hawkes[20], R.J. Hawkings[36], Y. Hayashi[154], S. Hayashida[111], D. Hayden[107], C. Hayes[106], R.L. Hayes[114], C.P. Hays[126], J.M. Hays[94], H.S. Hayward[92], F. He[62a], M. He[14a,14e], Y. He[138], Y. He[48], N.B. Heatley[94], V. Hedberg[98], A.L. Heggelund[125], N.D. Hehir[94,*], C. Heidegger[54], K.K. Heidegger[54], W.D. Heidorn[81], J. Heilman[34], S. Heim[48], T. Heim[17a], J.G. Heinlein[128], J.J. Heinrich[123], L. Heinrich[110,af], J. Hejbal[131], L. Helary[48], A. Held[170], S. Hellesund[16], C.M. Helling[164], S. Hellman[47a,47b], R.C.W. Henderson[91], L. Henkelmann[32], A.M. Henriques Correia[36], H. Herde[98], Y. Hernández Jiménez[146], L.M. Herrmann[24], T. Herrmann[50], G. Herten[54], R. Hertenberger[109], L. Hervas[36], M.E. Hesping[100], N.P. Hessey[156a], H. Hibi[85], E. Hill[155], S.J. Hillier[20], J.R. Hinds[107], F. Hinterkeuser[24], M. Hirose[124], S. Hirose[157],

D. Hirschbuehl[171], T.G. Hitchings[101], B. Hiti[93], J. Hobbs[146], R. Hobincu[27e], N. Hod[169], M.C. Hodgkinson[140], B.H. Hodkinson[32], A. Hoecker[36], D.D. Hofer[106], J. Hofer[48], T. Holm[24], M. Holzbock[110], L.B.A.H. Hommels[32], B.P. Honan[101], J. Hong[62c], T.M. Hong[129], B.H. Hooberman[162], W.H. Hopkins[6], Y. Horii[111], S. Hou[149], A.S. Howard[93], J. Howarth[59], J. Hoya[6], M. Hrabovsky[122], A. Hrynevich[48], T. Hryn'ova[4], P.J. Hsu[65], S.-C. Hsu[139], Q. Hu[62a], Y.F. Hu[14a,14e], S. Huang[64b], X. Huang[14c], X. Huang[14a,14e], Y. Huang[140], Y. Huang[14a], Z. Huang[101], Z. Hubacek[132], M. Huebner[24], F. Huegging[24], T.B. Huffman[126], C.A. Hugli[48], M. Huhtinen[36], S.K. Huiberts[16], R. Hulsken[104], N. Huseynov[12], J. Huston[107], J. Huth[61], R. Hyneman[144], G. Iacobucci[56], G. Iakovidis[29], I. Ibragimov[142], L. Iconomidou-Fayard[66], J.P. Iddon[36], P. Iengo[72a,72b], R. Iguchi[154], T. Iizawa[126], Y. Ikegami[84], N. Ilic[155], H. Imam[35a], M. Ince Lezki[56], T. Ingebretsen Carlson[47a,47b], G. Introzzi[73a,73b], M. Iodice[77a], V. Ippolito[75a,75b], R.K. Irwin[92], M. Ishino[154], W. Islam[170], C. Issever[18,48], S. Istin[21a,am], H. Ito[168], J.M. Iturbe Ponce[64a], R. Iuppa[78a,78b], A. Ivina[169], J.M. Izen[45], V. Izzo[72a], P. Jacka[131,132], P. Jackson[1], B.P. Jaeger[143], C.S. Jagfeld[109], G. Jain[156a], P. Jain[54], K. Jakobs[54], T. Jakoubek[169], J. Jamieson[59], K.W. Janas[86a], M. Javurkova[103], L. Jeanty[123], J. Jejelava[150a,ab], P. Jenni[54,g], C.E. Jessiman[34], S. Jézéquel[4], C. Jia[62b], J. Jia[146], X. Jia[61], X. Jia[14a,14e], Z. Jia[14c], S. Jiggins[48], J. Jimenez Pena[13], S. Jin[14c], A. Jinaru[27b], O. Jinnouchi[138], P. Johansson[140], K.A. Johns[7], J.W. Johnson[136], D.M. Jones[32], E. Jones[48], P. Jones[32], R.W.L. Jones[91], T.J. Jones[92], H.L. Joos[55,36], R. Joshi[119], J. Jovicevic[15], X. Ju[17a], J.J. Junggeburth[103], T. Junkermann[63a], A. Juste Rozas[13,u], M.K. Juzek[87], S. Kabana[137e], A. Kaczmarska[87], M. Kado[110], H. Kagan[119], M. Kagan[144], A. Kahn[41], A. Kahn[128], C. Kahra[100], T. Kaji[154], E. Kajomovitz[151], N. Kakati[169], I. Kalaitzidou[54], C.W. Kalderon[29], A. Kamenshchikov[155], N.J. Kang[136], D. Kar[33g], K. Karava[126], M.J. Kareem[156b], E. Karentzos[54], I. Karkanias[153], O. Karkout[114], S.N. Karpov[38], Z.M. Karpova[38], V. Kartvelishvili[91], A.N. Karyukhin[37], E. Kasimi[153], J. Katzy[48], S. Kaur[34], K. Kawade[141], M.P. Kawale[120], C. Kawamoto[88], T. Kawamoto[62a], E.F. Kay[36], F.I. Kaya[158], S. Kazakos[107], V.F. Kazanin[37], Y. Ke[146], J.M. Keaveney[33a], R. Keeler[165], G.V. Kehris[61], J.S. Keller[34], A.S. Kelly[96], J.J. Kempster[147], K.E. Kennedy[41], P.D. Kennedy[100], O. Kepka[131], B.P. Kerridge[167], S. Kersten[171], B.P. Kerševan[93], S. Keshri[66], L. Keszeghova[28a], S. Ketabchi Haghighat[155], R.A. Khan[129], A. Khanov[121], A.G. Kharlamov[37], T. Kharlamova[37], E.E. Khoda[139], M. Kholodenko[37], T.J. Khoo[18], G. Khoriauli[166], J. Khubua[150b,*], Y.A.R. Khwaira[66], A. Kilgallon[123], D.W. Kim[47a,47b], Y.K. Kim[39], N. Kimura[96], M.K. Kingston[55], A. Kirchhoff[55], C. Kirfel[24], F. Kirfel[24], J. Kirk[134], A.E. Kiryunin[110], C. Kitsaki[10], O. Kivernyk[24], M. Klassen[63a], C. Klein[34], L. Klein[166], M.H. Klein[44], M. Klein[92,*], S.B. Klein[56], U. Klein[92], P. Klimek[36], A. Klimentov[29], T. Klioutchnikova[36], P. Kluit[114], S. Kluth[110], E. Kneringer[79], T.M. Knight[155], A. Knue[49], R. Kobayashi[88], D. Kobylianskii[169], S.F. Koch[126], M. Kocian[144], P. Kodyš[133], D.M. Koeck[123], P.T. Koenig[24], T. Koffas[34], O. Kolay[50], I. Koletsou[4], T. Komarek[122], K. Köneke[54], A.X.Y. Kong[1], T. Kono[118], N. Konstantinidis[96], P. Kontaxakis[56], B. Konya[98], R. Kopeliansky[68], S. Koperny[86a], K. Korcyl[87], K. Kordas[153,e], A. Korn[96], S. Korn[55], I. Korolkov[13], N. Korotkova[37], B. Kortman[114], O. Kortner[110], S. Kortner[110],

JHEP01(2025)053

W.H. Kostecka[115], V.V. Kostyukhin[142], A. Kotsokechagia[135], A. Kotwal[51], A. Koulouris[36], A. Kourkoumeli-Charalampidi[73a,73b], C. Kourkoumelis[9], E. Kourlitis[110,af], O. Kovanda[147], R. Kowalewski[165], W. Kozanecki[135], A.S. Kozhin[37], V.A. Kramarenko[37], G. Kramberger[93], P. Kramer[100], M.W. Krasny[127], A. Krasznahorkay[36], J.W. Kraus[171], J.A. Kremer[48], T. Kresse[50], J. Kretzschmar[92], K. Kreul[18], P. Krieger[155], S. Krishnamurthy[103], M. Krivos[133], K. Krizka[20], K. Kroeninger[49], H. Kroha[110], J. Kroll[131], J. Kroll[128], K.S. Krowpman[107], U. Kruchonak[38], H. Krüger[24], N. Krumnack[81], M.C. Kruse[51], O. Kuchinskaia[37], S. Kuday[3a], S. Kuehn[36], R. Kuesters[54], T. Kuhl[48], V. Kukhtin[38], Y. Kulchitsky[37,a], S. Kuleshov[137d,137b], M. Kumar[33g], N. Kumari[48], P. Kumari[156b], A. Kupco[131], T. Kupfer[49], A. Kupich[37], O. Kuprash[54], H. Kurashige[85], L.L. Kurchaninov[156a], O. Kurdysh[66], Y.A. Kurochkin[37], A. Kurova[37], M. Kuze[138], A.K. Kvam[103], J. Kvita[122], T. Kwan[104], N.G. Kyriacou[106], L.A.O. Laatu[102], C. Lacasta[163], F. Lacava[75a,75b], H. Lacker[18], D. Lacour[127], N.N. Lad[96], E. Ladygin[38], B. Laforge[127], T. Lagouri[27b], F.Z. Lahbabi[35a], S. Lai[55], I.K. Lakomiec[86a], N. Lalloue[60], J.E. Lambert[165], S. Lammers[68], W. Lampl[7], C. Lampoudis[153,e], A.N. Lancaster[115], E. Lançon[29], U. Landgraf[54], M.P.J. Landon[94], V.S. Lang[54], R.J. Langenberg[103], O.K.B. Langrekken[125], A.J. Lankford[159], F. Lanni[36], K. Lantzsch[24], A. Lanza[73a], A. Lapertosa[57b,57a], J.F. Laporte[135], T. Lari[71a], F. Lasagni Manghi[23b], M. Lassnig[36], V. Latonova[131], A. Laudrain[100], A. Laurier[151], S.D. Lawlor[140], Z. Lawrence[101], R. Lazaridou[167], M. Lazzaroni[71a,71b], B. Le[101], E.M. Le Boulicaut[51], B. Leban[93], A. Lebedev[81], M. LeBlanc[101], F. Ledroit-Guillon[60], A.C.A. Lee[96], S.C. Lee[149], S. Lee[47a,47b], T.F. Lee[92], L.L. Leeuw[33c], H.P. Lefebvre[95], M. Lefebvre[165], C. Leggett[17a], G. Lehmann Miotto[36], M. Leigh[56], W.A. Leight[103], W. Leinonen[113], A. Leisos[153,t], M.A.L. Leite[83c], C.E. Leitgeb[18], R. Leitner[133], K.J.C. Leney[44], T. Lenz[24], S. Leone[74a], C. Leonidopoulos[52], A. Leopold[145], C. Leroy[108], R. Les[107], C.G. Lester[32], M. Levchenko[37], J. Levêque[4], D. Levin[106], L.J. Levinson[169], G. Levrini[23b,23a], M.P. Lewicki[87], D.J. Lewis[4], A. Li[5], B. Li[62b], C. Li[62a], C-Q. Li[110], H. Li[62a], H. Li[62b], H. Li[14c], H. Li[14b], H. Li[62b], J. Li[62c], K. Li[139], L. Li[62c], M. Li[14a,14e], Q.Y. Li[62a], S. Li[14a,14e], S. Li[62d,62c,d], T. Li[5], X. Li[104], Z. Li[126], Z. Li[104], Z. Li[14a,14e], S. Liang[14a,14e], Z. Liang[14a], M. Liberatore[135], B. Liberti[76a], K. Lie[64c], J. Lieber Marin[83b], H. Lien[68], K. Lin[107], R.E. Lindley[7], J.H. Lindon[2], E. Lipeles[128], A. Lipniacka[16], A. Lister[164], J.D. Little[4], B. Liu[14a], B.X. Liu[143], D. Liu[62d,62c], J.B. Liu[62a], J.K.K. Liu[32], K. Liu[62d,62c], M. Liu[62a], M.Y. Liu[62a], P. Liu[14a], Q. Liu[62d,139,62c], X. Liu[62a], X. Liu[62b], Y. Liu[14d,14e], Y.L. Liu[62b], Y.W. Liu[62a], J. Llorente Merino[143], S.L. Lloyd[94], E.M. Lobodzinska[48], P. Loch[7], T. Lohse[18], K. Lohwasser[140], E. Loiacono[48], M. Lokajicek[131,*], J.D. Lomas[20], J.D. Long[162], I. Longarini[159], L. Longo[70a,70b], R. Longo[162], I. Lopez Paz[67], A. Lopez Solis[48], N. Lorenzo Martinez[4], A.M. Lory[109], G. Löschcke Centeno[147], O. Loseva[37], X. Lou[47a,47b], X. Lou[14a,14e], A. Lounis[66], J. Love[6], P.A. Love[91], G. Lu[14a,14e], M. Lu[80], S. Lu[128], Y.J. Lu[65], H.J. Lubatti[139], C. Luci[75a,75b], F.L. Lucio Alves[14c], A. Lucotte[60], F. Luehring[68], I. Luise[146], O. Lukianchuk[66], O. Lundberg[145], B. Lund-Jensen[145,*], N.A. Luongo[6], M.S. Lutz[36], A.B. Lux[25], D. Lynn[29], H. Lyons[92], R. Lysak[131], E. Lytken[98], V. Lyubushkin[38], T. Lyubushkina[38], M.M. Lyukova[146], H. Ma[29], K. Ma[62a], L.L. Ma[62b], W. Ma[62a], Y. Ma[121], D.M. Mac Donell[165], G. Maccarrone[53], J.C. MacDonald[100], P.C. Machado De Abreu Farias[83b], R. Madar[40], W.F. Mader[50], T. Madula[96], J. Maeda[85], T. Maeno[29], H. Maguire[140], V. Maiboroda[135], A. Maio[130a,130b,130d], K. Maj[86a], O. Majersky[48], S. Majewski[123], N. Makovec[66], V. Maksimovic[15], B. Malaescu[127], Pa. Malecki[87], V.P. Maleev[37], F. Malek[60,o], M. Mali[93], D. Malito[95], U. Mallik[80,*], S. Maltezos[10], S. Malyukov[38], J. Mamuzic[13], G. Mancini[53], M.N. Mancini[26], G. Manco[73a,73b], J.P. Mandalia[94], I. Mandić[93], L. Manhaes de Andrade Filho[83a], I.M. Maniatis[169], J. Manjarres Ramos[102,ac], D.C. Mankad[169], A. Mann[109], S. Manzoni[36], L. Mao[62c], X. Mapekula[33c], A. Marantis[153,t], G. Marchiori[5], M. Marcisovsky[131], C. Marcon[71a], M. Marinescu[20], S. Marium[48], M. Marjanovic[120], E.J. Marshall[91], Z. Marshall[17a], S. Marti-Garcia[163], T.A. Martin[167], V.J. Martin[52], B. Martin dit Latour[16], L. Martinelli[75a,75b], M. Martinez[13,u], P. Martinez Agullo[163], V.I. Martinez Outschoorn[103], P. Martinez Suarez[13], S. Martin-Haugh[134], V.S. Martoiu[27b], A.C. Martyniuk[96], A. Marzin[36], D. Mascione[78a,78b], L. Masetti[100], T. Mashimo[154], J. Masik[101], A.L. Maslennikov[37], P. Massarotti[72a,72b], P. Mastrandrea[74a,74b], A. Mastroberardino[43b,43a], T. Masubuchi[154], T. Mathisen[161], J. Matousek[133], N. Matsuzawa[154], J. Maurer[27b], B. Maček[93], D.A. Maximov[37], R. Mazini[149], I. Maznas[153], M. Mazza[107], S.M. Mazza[136], E. Mazzeo[71a,71b], C. Mc Ginn[29], J.P. Mc Gowan[104], S.P. Mc Kee[106], C.C. McCracken[164], E.F. McDonald[105], A.E. McDougall[114], J.A. Mcfayden[147], R.P. McGovern[128], G. Mchedlidze[150b], R.P. Mckenzie[33g], T.C. Mclachlan[48], D.J. Mclaughlin[96], S.J. McMahon[134], C.M. Mcpartland[92], R.A. McPherson[165,y], S. Mehlhase[109], A. Mehta[92], D. Melini[163], B.R. Mellado Garcia[33g], A.H. Melo[55], F. Meloni[48], A.M. Mendes Jacques Da Costa[101], H.Y. Meng[155], L. Meng[91], S. Menke[110], M. Mentink[36], E. Meoni[43b,43a], G. Mercado[115], C. Merlassino[69a,69c], L. Merola[72a,72b], C. Meroni[71a,71b], J. Metcalfe[6], A.S. Mete[6], C. Meyer[68], J-P. Meyer[135], R.P. Middleton[134], L. Mijović[52], G. Mikenberg[169], M. Mikestikova[131], M. Mikuž[93], H. Mildner[100], A. Milic[36], C.D. Milke[44], D.W. Miller[39], E.H. Miller[144], L.S. Miller[34], A. Milov[169], D.A. Milstead[47a,47b], T. Min[14c], A.A. Minaenko[37], I.A. Minashvili[150b], L. Mince[59], A.I. Mincer[117], B. Mindur[86a], M. Mineev[38], Y. Mino[88], L.M. Mir[13], M. Miralles Lopez[59], M. Mironova[17a], A. Mishima[154], M.C. Missio[113], A. Mitra[167], V.A. Mitsou[163], Y. Mitsumori[111], O. Miu[155], P.S. Miyagawa[94], T. Mkrtchyan[63a], M. Mlinarevic[96], T. Mlinarevic[96], M. Mlynarikova[36], S. Mobius[19], P. Mogg[109], M.H. Mohamed Farook[112], A.F. Mohammed[14a,14e], S. Mohapatra[41], G. Mokgatitswane[33g], L. Moleri[169], B. Mondal[142], S. Mondal[132], K. Mönig[48], E. Monnier[102], L. Monsonis Romero[163], J. Montejo Berlingen[13], M. Montella[119], F. Montereali[77a,77b], F. Monticelli[90], S. Monzani[69a,69c], N. Morange[66], A.L. Moreira De Carvalho[130a], M. Moreno Llácer[163], C. Moreno Martinez[56], P. Morettini[57b], S. Morgenstern[36], M. Morii[61], M. Morinaga[154], A.K. Morley[36], F. Morodei[75a,75b], L. Morvaj[36], P. Moschovakos[36], B. Moser[36], M. Mosidze[150b], T. Moskalets[54], P. Moskvitina[113], J. Moss[31,l], E.J.W. Moyse[103], O. Mtintsilana[33g], S. Muanza[102], J. Mueller[129], D. Muenstermann[91], R. Müller[19], G.A. Mullier[161], A.J. Mullin[32], J.J. Mullin[128], D.P. Mungo[155], D. Munoz Perez[163], F.J. Munoz Sanchez[101], M. Murin[101], W.J. Murray[167,134], A. Murrone[71a,71b], M. Muškinja[17a], C. Mwewa[29], A.G. Myagkov[37,a], A.J. Myers[8], G. Myers[68], M. Myska[132], B.P. Nachman[17a], O. Nackenhorst[49], K. Nagai[126], K. Nagano[84], J.L. Nagle[29,ak], E. Nagy[102], A.M. Nairz[36], Y. Nakahama[84], K. Nakamura[84], K. Nakkalil[5], H. Nanjo[124], R. Narayan[44], E.A. Narayanan[112], I. Naryshkin[37], M. Naseri[34], S. Nasri[116b], C. Nass[24], G. Navarro[22a], J. Navarro-Gonzalez[163], R. Nayak[152], A. Nayaz[18], P.Y. Nechaeva[37], F. Nechansky[48], L. Nedic[126], T.J. Neep[20], A. Negri[73a,73b], M. Negrini[23b], C. Nellist[114], C. Nelson[104], K. Nelson[106], S. Nemecek[131], M. Nessi[36,h], M.S. Neubauer[162], F. Neuhaus[100], J. Neundorf[48], R. Newhouse[164], P.R. Newman[20], C.W. Ng[129], Y.W.Y. Ng[48], B. Ngair[116a], H.D.N. Nguyen[108], R.B. Nickerson[126], R. Nicolaidou[135], J. Nielsen[136], M. Niemeyer[55], J. Niermann[55,36], N. Nikiforou[36], V. Nikolaenko[37,a], I. Nikolic-Audit[127], K. Nikolopoulos[20], P. Nilsson[29], I. Ninca[48], H.R. Nindhito[56], G. Ninio[152], A. Nisati[75a], N. Nishu[2], R. Nisius[110], J-E. Nitschke[50], E.K. Nkadimeng[33g], T. Nobe[154], D.L. Noel[32], T. Nommensen[148], M.B. Norfolk[140], R.R.B. Norisam[96], B.J. Norman[34], M. Noury[35a], J. Novak[93], T. Novak[48], L. Novotny[132], R. Novotny[112], L. Nozka[122], K. Ntekas[159], N.M.J. Nunes De Moura Junior[83b], E. Nurse[96], J. Ocariz[127], A. Ochi[85], I. Ochoa[130a], S. Oerdek[48,v], J.T. Offermann[39], A. Ogrodnik[133], A. Oh[101], C.C. Ohm[145], H. Oide[84], R. Oishi[154], M.L. Ojeda[48], Y. Okumura[154], L.F. Oleiro Seabra[130a], S.A. Olivares Pino[137d], D. Oliveira Damazio[29], D. Oliveira Goncalves[83a], J.L. Oliver[159], Ö.O. Öncel[54], A.P. O'Neill[19], A. Onofre[130a,130e], P.U.E. Onyisi[11], M.J. Oreglia[39], G.E. Orellana[90], D. Orestano[77a,77b], N. Orlando[13], R.S. Orr[155], V. O'Shea[59], L.M. Osojnak[128], R. Ospanov[62a], G. Otero y Garzon[30], H. Otono[89], P.S. Ott[63a], G.J. Ottino[17a], M. Ouchrif[35d], F. Ould-Saada[125], M. Owen[59], R.E. Owen[134], K.Y. Oyulmaz[21a], V.E. Ozcan[21a], F. Ozturk[87], N. Ozturk[8], S. Ozturk[82], H.A. Pacey[126], A. Pacheco Pages[13], C. Padilla Aranda[13], G. Padovano[75a,75b], S. Pagan Griso[17a], G. Palacino[68], A. Palazzo[70a,70b], J. Pan[172], T. Pan[64a], D.K. Panchal[11], C.E. Pandini[114], J.G. Panduro Vazquez[95], H.D. Pandya[1], H. Pang[14b], P. Pani[48], G. Panizzo[69a,69c], L. Paolozzi[56], C. Papadatos[108], S. Parajuli[162], A. Paramonov[6], C. Paraskevopoulos[53], D. Paredes Hernandez[64b], K.R. Park[41], T.H. Park[155], M.A. Parker[32], F. Parodi[57b,57a], E.W. Parrish[115], V.A. Parrish[52], J.A. Parsons[41], U. Parzefall[54], B. Pascual Dias[108], L. Pascual Dominguez[152], E. Pasqualucci[75a], S. Passaggio[57b], F. Pastore[95], P. Pasuwan[47a,47b], P. Patel[87], U.M. Patel[51], J.R. Pater[101], T. Pauly[36], J. Pearkes[144], M. Pedersen[125], R. Pedro[130a], S.V. Peleganchuk[37], O. Penc[36], E.A. Pender[52], K.E. Penski[109], M. Penzin[37], B.S. Peralva[83d], A.P. Pereira Peixoto[60], L. Pereira Sanchez[47a,47b], D.V. Perepelitsa[29,ak], E. Perez Codina[156a], M. Perganti[10], H. Pernegger[36], O. Perrin[40], K. Peters[48], R.F.Y. Peters[101], B.A. Petersen[36], T.C. Petersen[42], E. Petit[102], V. Petousis[132], C. Petridou[153,e], A. Petrukhin[142], M. Pettee[17a], N.E. Pettersson[36], A. Petukhov[37], K. Petukhova[133], R. Pezoa[137f], L. Pezzotti[36], G. Pezzullo[172], T.M. Pham[170], T. Pham[105], P.W. Phillips[134], G. Piacquadio[146], E. Pianori[17a], F. Piazza[123], R. Piegaia[30], D. Pietreanu[27b], A.D. Pilkington[101], M. Pinamonti[69a,69c], J.L. Pinfold[2], B.C. Pinheiro Pereira[130a], A.E. Pinto Pinoargote[100,135], L. Pintucci[69a,69c], K.M. Piper[147], A. Pirttikoski[56], D.A. Pizzi[34], L. Pizzimento[64b], A. Pizzini[114], M.-A. Pleier[29], V. Plesanovs[54], V. Pleskot[133], E. Plotnikova[38], G. Poddar[4], R. Poettgen[98], L. Poggioli[127], I. Pokharel[55],

S. Polacek[133], G. Polesello[73a], A. Poley[143,156a], R. Polifka[132], A. Polini[23b], C.S. Pollard[167], Z.B. Pollock[119], V. Polychronakos[29], E. Pompa Pacchi[75a,75b], D. Ponomarenko[113], L. Pontecorvo[36], S. Popa[27a], G.A. Popeneciu[27d], A. Poreba[36], D.M. Portillo Quintero[156a], S. Pospisil[132], M.A. Postill[140], P. Postolache[27c], K. Potamianos[167], P.A. Potepa[86a], I.N. Potrap[38], C.J. Potter[32], H. Potti[1], T. Poulsen[48], J. Poveda[163], M.E. Pozo Astigarraga[36], A. Prades Ibanez[163], J. Pretel[54], D. Price[101], M. Primavera[70a], M.A. Principe Martin[99], R. Privara[122], T. Procter[59], M.L. Proffitt[139], N. Proklova[128], K. Prokofiev[64c], G. Proto[110], S. Protopopescu[29], J. Proudfoot[6], M. Przybycien[86a], W.W. Przygoda[86b], A. Psallidas[46], J.E. Puddefoot[140], D. Pudzha[37], D. Pyatiizbyantseva[37], J. Qian[106], D. Qichen[101], Y. Qin[101], T. Qiu[52], A. Quadt[55], M. Queitsch-Maitland[101], G. Quetant[56], R.P. Quinn[164], G. Rabanal Bolanos[61], D. Rafanoharana[54], F. Ragusa[71a,71b], J.L. Rainbolt[39], J.A. Raine[56], S. Rajagopalan[29], E. Ramakoti[37], I.A. Ramirez-Berend[34], K. Ran[48,14e], N.P. Rapheeha[33g], H. Rasheed[27b], V. Raskina[127], D.F. Rassloff[63a], A. Rastogi[17a], S. Rave[100], B. Ravina[55], I. Ravinovich[169], M. Raymond[36], A.L. Read[125], N.P. Readioff[140], D.M. Rebuzzi[73a,73b], G. Redlinger[29], A.S. Reed[110], K. Reeves[26], J.A. Reidelsturz[171], D. Reikher[152], A. Rej[49], C. Rembser[36], A. Renardi[48], M. Renda[27b], M.B. Rendel[110], F. Renner[48], A.G. Rennie[159], A.L. Rescia[48], S. Resconi[71a], M. Ressegotti[57b,57a], S. Rettie[36], J.G. Reyes Rivera[107], E. Reynolds[17a], O.L. Rezanova[37], P. Reznicek[133], N. Ribaric[91], E. Ricci[78a,78b], R. Richter[110], S. Richter[47a,47b], E. Richter-Was[86b], M. Ridel[127], S. Ridouani[35d], P. Rieck[117], P. Riedler[36], E.M. Riefel[47a,47b], J.O. Rieger[114], M. Rijssenbeek[146], A. Rimoldi[73a,73b], M. Rimoldi[36], L. Rinaldi[23b,23a], T.T. Rinn[29], M.P. Rinnagel[109], G. Ripellino[161], I. Riu[13], P. Rivadeneira[48], J.C. Rivera Vergara[165], F. Rizatdinova[121], E. Rizvi[94], B.A. Roberts[167], B.R. Roberts[17a], S.H. Robertson[104,y], D. Robinson[32], C.M. Robles Gajardo[137f], M. Robles Manzano[100], A. Robson[59], A. Rocchi[76a,76b], C. Roda[74a,74b], S. Rodriguez Bosca[63a], Y. Rodriguez Garcia[22a], A. Rodriguez Rodriguez[54], A.M. Rodríguez Vera[156b], S. Roe[36], J.T. Roemer[159], A.R. Roepe-Gier[136], J. Roggel[171], O. Røhne[125], R.A. Rojas[103], C.P.A. Roland[127], J. Roloff[29], A. Romaniouk[37], E. Romano[73a,73b], M. Romano[23b], A.C. Romero Hernandez[162], N. Rompotis[92], L. Roos[127], S. Rosati[75a], B.J. Rosser[39], E. Rossi[126], E. Rossi[72a,72b], L.P. Rossi[57b], L. Rossini[54], R. Rosten[119], M. Rotaru[27b], B. Rottler[54], C. Rougier[102,ac], D. Rousseau[66], D. Rousso[32], A. Roy[162], S. Roy-Garand[155], A. Rozanov[102], Z.M.A. Rozario[59], Y. Rozen[151], X. Ruan[33g], A. Rubio Jimenez[163], A.J. Ruby[92], V.H. Ruelas Rivera[18], T.A. Ruggeri[1], A. Ruggiero[126], A. Ruiz-Martinez[163], A. Rummler[36], Z. Rurikova[54], N.A. Rusakovich[38], H.L. Russell[165], G. Russo[75a,75b], J.P. Rutherfoord[7], S. Rutherford Colmenares[32], K. Rybacki[91], M. Rybar[133], E.B. Rye[125], A. Ryzhov[44], J.A. Sabater Iglesias[56], P. Sabatini[163], H.F-W. Sadrozinski[136], F. Safai Tehrani[75a], B. Safarzadeh Samani[134], M. Safdari[144], S. Saha[165], M. Sahinsoy[110], A. Saibel[163], M. Saimpert[135], M. Saito[154], T. Saito[154], D. Salamani[36], A. Salnikov[144], J. Salt[163], A. Salvador Salas[152], D. Salvatore[43b,43a], F. Salvatore[147], A. Salzburger[36], D. Sammel[54], D. Sampsonidis[153,e], D. Sampsonidou[123], J. Sánchez[163], A. Sanchez Pineda[4], V. Sanchez Sebastian[163], H. Sandaker[125], C.O. Sander[48], J.A. Sandesara[103], M. Sandhoff[171], C. Sandoval[22b], D.P.C. Sankey[134], T. Sano[88], A. Sansoni[53], L. Santi[75a,75b], C. Santoni[40],

H. Santos[130a,130b], A. Santra[169], K.A. Saoucha[160], J.G. Saraiva[130a,130d], J. Sardain[7], O. Sasaki[84], K. Sato[157], C. Sauer[63b], F. Sauerburger[54], E. Sauvan[4], P. Savard[155,ah], R. Sawada[154], C. Sawyer[134], L. Sawyer[97], I. Sayago Galvan[163], C. Sbarra[23b], A. Sbrizzi[23b,23a], T. Scanlon[96], J. Schaarschmidt[139], U. Schäfer[100], A.C. Schaffer[66,44], D. Schaile[109], R.D. Schamberger[146], C. Scharf[18], M.M. Schefer[19], V.A. Schegelsky[37], D. Scheirich[133], F. Schenck[18], M. Schernau[159], C. Scheulen[55], C. Schiavi[57b,57a], E.J. Schioppa[70a,70b], M. Schioppa[43b,43a], B. Schlag[144], K.E. Schleicher[54], S. Schlenker[36], J. Schmeing[171], M.A. Schmidt[171], K. Schmieden[100], C. Schmitt[100], N. Schmitt[100], S. Schmitt[48], L. Schoeffel[135], A. Schoening[63b], P.G. Scholer[54], E. Schopf[126], M. Schott[100], J. Schovancova[36], S. Schramm[56], F. Schroeder[171], T. Schroer[56], H-C. Schultz-Coulon[63a], M. Schumacher[54], B.A. Schumm[136], Ph. Schune[135], A.J. Schuy[139], H.R. Schwartz[136], A. Schwartzman[144], T.A. Schwarz[106], Ph. Schwemling[135], R. Schwienhorst[107], A. Sciandra[136], G. Sciolla[26], F. Scuri[74a], C.D. Sebastiani[92], K. Sedlaczek[115], P. Seema[18], S.C. Seidel[112], A. Seiden[136], B.D. Seidlitz[41], C. Seitz[48], J.M. Seixas[83b], G. Sekhniaidze[72a], L. Selem[60], N. Semprini-Cesari[23b,23a], D. Sengupta[56], V. Senthilkumar[163], L. Serin[66], L. Serkin[69a,69b], M. Sessa[76a,76b], H. Severini[120], F. Sforza[57b,57a], A. Sfyrla[56], E. Shabalina[55], R. Shaheen[145], J.D. Shahinian[128], D. Shaked Renous[169], L.Y. Shan[14a], M. Shapiro[17a], A. Sharma[36], A.S. Sharma[164], P. Sharma[80], S. Sharma[48], P.B. Shatalov[37], K. Shaw[147], S.M. Shaw[101], A. Shcherbakova[37], Q. Shen[62c,5], D.J. Sheppard[143], P. Sherwood[96], L. Shi[96], X. Shi[14a], C.O. Shimmin[172], J.D. Shinner[95], I.P.J. Shipsey[126,*], S. Shirabe[89], M. Shiyakova[38,w], J. Shlomi[169], M.J. Shochet[39], J. Shojaii[105], D.R. Shope[125], B. Shrestha[120], S. Shrestha[119,al], E.M. Shrif[33g], M.J. Shroff[165], P. Sicho[131], A.M. Sickles[162], E. Sideras Haddad[33g], A. Sidoti[23b], F. Siegert[50], Dj. Sijacki[15], F. Sili[90], J.M. Silva[20], M.V. Silva Oliveira[29], S.B. Silverstein[47a], S. Simion[66], R. Simoniello[36], E.L. Simpson[59], H. Simpson[147], L.R. Simpson[106], N.D. Simpson[98], S. Simsek[82], S. Sindhu[55], P. Sinervo[155], S. Singh[155], S. Sinha[48], S. Sinha[101], M. Sioli[23b,23a], I. Siral[36], E. Sitnikova[48], S.Yu. Sivoklokov[37,*], J. Sjölin[47a,47b], A. Skaf[55], E. Skorda[20], P. Skubic[120], M. Slawinska[87], V. Smakhtin[169], B.H. Smart[134], S.Yu. Smirnov[37], Y. Smirnov[37], L.N. Smirnova[37,a], O. Smirnova[98], A.C. Smith[41], E.A. Smith[39], H.A. Smith[126], J.L. Smith[92], R. Smith[144], M. Smizanska[91], K. Smolek[132], A.A. Snesarev[37], S.R. Snider[155], H.L. Snoek[114], S. Snyder[29], R. Sobie[165,y], A. Soffer[152], C.A. Solans Sanchez[36], E.Yu. Soldatov[37], U. Soldevila[163], A.A. Solodkov[37], S. Solomon[26], A. Soloshenko[38], K. Solovieva[54], O.V. Solovyanov[40], V. Solovyev[37], P. Sommer[36], A. Sonay[13], W.Y. Song[156b], A. Sopczak[132], A.L. Sopio[96], F. Sopkova[28b], J.D. Sorenson[112], I.R. Sotarriva Alvarez[138], V. Sothilingam[63a], O.J. Soto Sandoval[137c,137b], S. Sottocornola[68], R. Soualah[160], Z. Soumaimi[35e], D. South[48], N. Soybelman[169], S. Spagnolo[70a,70b], M. Spalla[110], D. Sperlich[54], G. Spigo[36], S. Spinali[91], D.P. Spiteri[59], M. Spousta[133], E.J. Staats[34], R. Stamen[63a], A. Stampekis[20], M. Standke[24], E. Stanecka[87], M.V. Stange[50], B. Stanislaus[17a], M.M. Stanitzki[48], B. Stapf[48], E.A. Starchenko[37], G.H. Stark[136], J. Stark[102,ac], P. Staroba[131], P. Starovoitov[63a], S. Stärz[104], R. Staszewski[87], G. Stavropoulos[46], J. Steentoft[161], P. Steinberg[29], B. Stelzer[143,156a], H.J. Stelzer[129], O. Stelzer-Chilton[156a], H. Stenzel[58], T.J. Stevenson[147], G.A. Stewart[36],

JHEP01(2025)053

J.R. Stewart[121], M.C. Stockton[36], G. Stoicea[27b], M. Stolarski[130a], S. Stonjek[110], A. Straessner[50], J. Strandberg[145], S. Strandberg[47a,47b], M. Stratmann[171], M. Strauss[120], T. Strebler[102], P. Strizenec[28b], R. Ströhmer[166], D.M. Strom[123], R. Stroynowski[44], A. Strubig[47a,47b], S.A. Stucci[29], B. Stugu[16], J. Stupak[120], N.A. Styles[48], D. Su[144], S. Su[62a], W. Su[62d], X. Su[62a,66], K. Sugizaki[154], V.V. Sulin[37], M.J. Sullivan[92], D.M.S. Sultan[78a,78b], L. Sultanaliyeva[37], S. Sultansoy[3b], T. Sumida[88], S. Sun[106], S. Sun[170], O. Sunneborn Gudnadottir[161], N. Sur[102], M.R. Sutton[147], H. Suzuki[157], M. Svatos[131], M. Swiatlowski[156a], T. Swirski[166], I. Sykora[28a], M. Sykora[133], T. Sykora[133], D. Ta[100], K. Tackmann[48,v], A. Taffard[159], R. Tafirout[156a], J.S. Tafoya Vargas[66], E.P. Takeva[52], Y. Takubo[84], M. Talby[102], A.A. Talyshev[37], K.C. Tam[64b], N.M. Tamir[152], A. Tanaka[154], J. Tanaka[154], R. Tanaka[66], M. Tanasini[57b,57a], Z. Tao[164], S. Tapia Araya[137f], S. Tapprogge[100], A. Tarek Abouelfadl Mohamed[107], S. Tarem[151], K. Tariq[14a], G. Tarna[102,27b], G.F. Tartarelli[71a], P. Tas[133], M. Tasevsky[131], E. Tassi[43b,43a], A.C. Tate[162], G. Tateno[154], Y. Tayalati[35e,x], G.N. Taylor[105], W. Taylor[156b], A.S. Tee[170], R. Teixeira De Lima[144], P. Teixeira-Dias[95], J.J. Teoh[155], K. Terashi[154], J. Terron[99], S. Terzo[13], M. Testa[53], R.J. Teuscher[155,y], A. Thaler[79], O. Theiner[56], N. Themistokleous[52], T. Theveneaux-Pelzer[102], O. Thielmann[171], D.W. Thomas[95], J.P. Thomas[20], E.A. Thompson[17a], P.D. Thompson[20], E. Thomson[128], Y. Tian[55], V. Tikhomirov[37,a], Yu.A. Tikhonov[37], S. Timoshenko[37], D. Timoshyn[133], E.X.L. Ting[1], P. Tipton[172], S.H. Tlou[33g], A. Tnourji[40], K. Todome[138], S. Todorova-Nova[133], S. Todt[50], M. Togawa[84], J. Tojo[89], S. Tokár[28a], K. Tokushuku[84], O. Toldaiev[68], R. Tombs[32], M. Tomoto[84,111], L. Tompkins[144,n], K.W. Topolnicki[86b], E. Torrence[123], H. Torres[102,ac], E. Torró Pastor[163], M. Toscani[30], C. Tosciri[39], M. Tost[11], D.R. Tovey[140], A. Traeet[16], I.S. Trandafir[27b], T. Trefzger[166], A. Tricoli[29], I.M. Trigger[156a], S. Trincaz-Duvoid[127], D.A. Trischuk[26], B. Trocmé[60], C. Troncon[71a], L. Truong[33c], M. Trzebinski[87], A. Trzupek[87], F. Tsai[146], M. Tsai[106], A. Tsiamis[153,e], P.V. Tsiareshka[37], S. Tsigaridas[156a], A. Tsirigotis[153,t], V. Tsiskaridze[155], E.G. Tskhadadze[150a], M. Tsopoulou[153,e], Y. Tsujikawa[88], I.I. Tsukerman[37], V. Tsulaia[17a], S. Tsuno[84], K. Tsuri[118], D. Tsybychev[146], Y. Tu[64b], A. Tudorache[27b], V. Tudorache[27b], A.N. Tuna[61], S. Turchikhin[57b,57a], I. Turk Cakir[3a], R. Turra[71a], T. Turtuvshin[38,z], P.M. Tuts[41], S. Tzamarias[153,e], P. Tzanis[10], E. Tzovara[100], F. Ukegawa[157], P.A. Ulloa Poblete[137c,137b], E.N. Umaka[29], G. Unal[36], M. Unal[11], A. Undrus[29], G. Unel[159], J. Urban[28b], P. Urquijo[105], P. Urrejola[137a], G. Usai[8], R. Ushioda[138], M. Usman[108], Z. Uysal[82], V. Vacek[132], B. Vachon[104], K.O.H. Vadla[125], T. Vafeiadis[36], A. Vaitkus[96], C. Valderanis[109], E. Valdes Santurio[47a,47b], M. Valente[156a], S. Valentinetti[23b,23a], A. Valero[163], E. Valiente Moreno[163], A. Vallier[102,ac], J.A. Valls Ferrer[163], D.R. Van Arneman[114], T.R. Van Daalen[139], A. Van Der Graaf[49], P. Van Gemmeren[6], M. Van Rijnbach[125,36], S. Van Stroud[96], I. Van Vulpen[114], M. Vanadia[76a,76b], W. Vandelli[36], E.R. Vandewall[121], D. Vannicola[152], L. Vannoli[57b,57a], R. Vari[75a], E.W. Varnes[7], C. Varni[17b], T. Varol[149], D. Varouchas[66], L. Varriale[163], K.E. Varvell[148], M.E. Vasile[27b], L. Vaslin[84], G.A. Vasquez[165], A. Vasyukov[38], F. Vazeille[40], T. Vazquez Schroeder[36], J. Veatch[31], V. Vecchio[101], M.J. Veen[103], I. Veliscek[126], L.M. Veloce[155], F. Veloso[130a,130c], S. Veneziano[75a], A. Ventura[70a,70b],

JHEP01(2025)053

S. Ventura Gonzalez[135], A. Verbytskyi[110], M. Verducci[74a,74b], C. Vergis[24], M. Verissimo De Araujo[83b], W. Verkerke[114], J.C. Vermeulen[114], C. Vernieri[144], M. Vessella[103], M.C. Vetterli[143,ah], A. Vgenopoulos[153,e], N. Viaux Maira[137f], T. Vickey[140], O.E. Vickey Boeriu[140], G.H.A. Viehhauser[126], L. Vigani[63b], M. Villa[23b,23a], M. Villaplana Perez[163], E.M. Villhauer[52], E. Vilucchi[53], M.G. Vincter[34], G.S. Virdee[20], A. Vishwakarma[52], A. Visibile[114], C. Vittori[36], I. Vivarelli[147], E. Voevodina[110], F. Vogel[109], J.C. Voigt[50], P. Vokac[132], Yu. Volkotrub[86a], J. Von Ahnen[48], E. Von Toerne[24], B. Vormwald[36], V. Vorobel[133], K. Vorobev[37], M. Vos[163], K. Voss[142], J.H. Vossebeld[92], M. Vozak[114], L. Vozdecky[94], N. Vranjes[15], M. Vranjes Milosavljevic[15], M. Vreeswijk[114], N.K. Vu[62d,62c], R. Vuillermet[36], O. Vujinovic[100], I. Vukotic[39], S. Wada[157], C. Wagner[103], J.M. Wagner[17a], W. Wagner[171], S. Wahdan[171], H. Wahlberg[90], M. Wakida[111], J. Walder[134], R. Walker[109], W. Walkowiak[142], A. Wall[128], T. Wamorkar[6], A.Z. Wang[136], C. Wang[100], C. Wang[11], H. Wang[17a], J. Wang[64c], R.-J. Wang[100], R. Wang[61], R. Wang[6], S.M. Wang[149], S. Wang[62b], T. Wang[62a], W.T. Wang[80], W. Wang[14a], X. Wang[14c], X. Wang[162], X. Wang[62c], Y. Wang[62d], Y. Wang[14c], Z. Wang[106], Z. Wang[62d,51,62c], Z. Wang[106], A. Warburton[104], R.J. Ward[20], N. Warrack[59], S. Waterhouse[95], A.T. Watson[20], H. Watson[59], M.F. Watson[20], E. Watton[59,134], G. Watts[139], B.M. Waugh[96], C. Weber[29], H.A. Weber[18], M.S. Weber[19], S.M. Weber[63a], C. Wei[62a], Y. Wei[126], A.R. Weidberg[126], E.J. Weik[117], J. Weingarten[49], M. Weirich[100], C. Weiser[54], C.J. Wells[48], T. Wenaus[29], B. Wendland[49], T. Wengler[36], N.S. Wenke[110], N. Wermes[24], M. Wessels[63a], A.M. Wharton[91], A.S. White[61], A. White[8], M.J. White[1], D. Whiteson[159], L. Wickremasinghe[124], W. Wiedenmann[170], M. Wielers[134], C. Wiglesworth[42], D.J. Wilbern[120], H.G. Wilkens[36], D.M. Williams[41], H.H. Williams[128], S. Williams[32], S. Willocq[103], B.J. Wilson[101], P.J. Windischhofer[39], F.I. Winkel[30], F. Winklmeier[123], B.T. Winter[54], J.K. Winter[101], M. Wittgen[144], M. Wobisch[97], Z. Wolffs[114], J. Wollrath[159], M.W. Wolter[87], H. Wolters[130a,130c], A.F. Wongel[48], E.L. Woodward[41], S.D. Worm[48], B.K. Wosiek[87], K.W. Woźniak[87], S. Wozniewski[55], K. Wraight[59], C. Wu[20], J. Wu[14a,14e], M. Wu[64a], M. Wu[113], S.L. Wu[170], X. Wu[56], Y. Wu[62a], Z. Wu[135], J. Wuerzinger[110,af], T.R. Wyatt[101], B.M. Wynne[52], S. Xella[42], L. Xia[14c], M. Xia[14b], J. Xiang[64c], M. Xie[62a], X. Xie[62a], S. Xin[14a,14e], A. Xiong[123], J. Xiong[17a], D. Xu[14a], H. Xu[62a], L. Xu[62a], R. Xu[128], T. Xu[106], Y. Xu[14b], Z. Xu[52], Z. Xu[14c], B. Yabsley[148], S. Yacoob[33a], Y. Yamaguchi[138], E. Yamashita[154], H. Yamauchi[157], T. Yamazaki[17a], Y. Yamazaki[85], J. Yan[62c], S. Yan[126], Z. Yan[25], H.J. Yang[62c,62d], H.T. Yang[62a], S. Yang[62a], T. Yang[64c], X. Yang[36], X. Yang[14a], Y. Yang[44], Y. Yang[62a], Z. Yang[62a], W-M. Yao[17a], Y.C. Yap[48], H. Ye[14c], H. Ye[55], J. Ye[14a], S. Ye[29], X. Ye[62a], Y. Yeh[96], I. Yeletskikh[38], B. Yeo[17b], M.R. Yexley[96], P. Yin[41], K. Yorita[168], S. Younas[27b], C.J.S. Young[36], C. Young[144], C. Yu[14a,14e,aj], Y. Yu[62a], M. Yuan[106], R. Yuan[62b], L. Yue[96], M. Zaazoua[62a], B. Zabinski[87], E. Zaid[52], Z.K. Zak[87], T. Zakareishvili[163], N. Zakharchuk[34], S. Zambito[56], J.A. Zamora Saa[137d,137b], J. Zang[154], D. Zanzi[54], O. Zaplatilek[132], C. Zeitnitz[171], H. Zeng[14a], J.C. Zeng[162], D.T. Zenger Jr[26], O. Zenin[37], T. Ženiš[28a], S. Zenz[94], S. Zerradi[35a], D. Zerwas[66], M. Zhai[14a,14e], B. Zhang[14c], D.F. Zhang[140], J. Zhang[62b], J. Zhang[6], K. Zhang[14a,14e], L. Zhang[14c], P. Zhang[14a,14e], R. Zhang[170], S. Zhang[106], S. Zhang[44], T. Zhang[154],

JHEP01(2025)053

X. Zhang[62c], X. Zhang[62b], Y. Zhang[62c,5], Y. Zhang[96], Y. Zhang[14c], Z. Zhang[17a], Z. Zhang[66], H. Zhao[139], T. Zhao[62b], Y. Zhao[136], Z. Zhao[62a], A. Zhemchugov[38], J. Zheng[14c], K. Zheng[162], X. Zheng[62a], Z. Zheng[144], D. Zhong[162], B. Zhou[106], H. Zhou[7], N. Zhou[62c], Y. Zhou[14c], Y. Zhou[7], C.G. Zhu[62b], J. Zhu[106], Y. Zhu[62c], Y. Zhu[62a], X. Zhuang[14a], K. Zhukov[37], V. Zhulanov[37], N.I. Zimine[38], J. Zinsser[63b], M. Ziolkowski[142], L. Živković[15], A. Zoccoli[23b,23a], K. Zoch[61], T.G. Zorbas[140], O. Zormpa[46], W. Zou[41], L. Zwalinski[36]

[1] *Department of Physics, University of Adelaide, Adelaide; Australia*
[2] *Department of Physics, University of Alberta, Edmonton AB; Canada*
[3] [(a)] *Department of Physics, Ankara University, Ankara;*[(b)] *Division of Physics, TOBB University of Economics and Technology, Ankara; Türkiye*
[4] *LAPP, Université Savoie Mont Blanc, CNRS/IN2P3, Annecy; France*
[5] *APC, Université Paris Cité, CNRS/IN2P3, Paris; France*
[6] *High Energy Physics Division, Argonne National Laboratory, Argonne IL; United States of America*
[7] *Department of Physics, University of Arizona, Tucson AZ; United States of America*
[8] *Department of Physics, University of Texas at Arlington, Arlington TX; United States of America*
[9] *Physics Department, National and Kapodistrian University of Athens, Athens; Greece*
[10] *Physics Department, National Technical University of Athens, Zografou; Greece*
[11] *Department of Physics, University of Texas at Austin, Austin TX; United States of America*
[12] *Institute of Physics, Azerbaijan Academy of Sciences, Baku; Azerbaijan*
[13] *Institut de Física d'Altes Energies (IFAE), Barcelona Institute of Science and Technology, Barcelona; Spain*
[14] [(a)] *Institute of High Energy Physics, Chinese Academy of Sciences, Beijing;*[(b)] *Physics Department, Tsinghua University, Beijing;*[(c)] *Department of Physics, Nanjing University, Nanjing;*[(d)] *School of Science, Shenzhen Campus of Sun Yat-sen University;*[(e)] *University of Chinese Academy of Science (UCAS), Beijing; China*
[15] *Institute of Physics, University of Belgrade, Belgrade; Serbia*
[16] *Department for Physics and Technology, University of Bergen, Bergen; Norway*
[17] [(a)] *Physics Division, Lawrence Berkeley National Laboratory, Berkeley CA;*[(b)] *University of California, Berkeley CA; United States of America*
[18] *Institut für Physik, Humboldt Universität zu Berlin, Berlin; Germany*
[19] *Albert Einstein Center for Fundamental Physics and Laboratory for High Energy Physics, University of Bern, Bern; Switzerland*
[20] *School of Physics and Astronomy, University of Birmingham, Birmingham; United Kingdom*
[21] [(a)] *Department of Physics, Bogazici University, Istanbul;*[(b)] *Department of Physics Engineering, Gaziantep University, Gaziantep;*[(c)] *Department of Physics, Istanbul University, Istanbul; Türkiye*
[22] [(a)] *Facultad de Ciencias y Centro de Investigaciónes, Universidad Antonio Nariño, Bogotá;*[(b)] *Departamento de Física, Universidad Nacional de Colombia, Bogotá; Colombia*
[23] [(a)] *Dipartimento di Fisica e Astronomia A. Righi, Università di Bologna, Bologna;*[(b)] *INFN Sezione di Bologna; Italy*
[24] *Physikalisches Institut, Universität Bonn, Bonn; Germany*
[25] *Department of Physics, Boston University, Boston MA; United States of America*
[26] *Department of Physics, Brandeis University, Waltham MA; United States of America*
[27] [(a)] *Transilvania University of Brasov, Brasov;*[(b)] *Horia Hulubei National Institute of Physics and Nuclear Engineering, Bucharest;*[(c)] *Department of Physics, Alexandru Ioan Cuza University of Iasi, Iasi;*[(d)] *National Institute for Research and Development of Isotopic and Molecular Technologies, Physics Department, Cluj-Napoca;*[(e)] *National University of Science and Technology Politechnica, Bucharest;*[(f)] *West University in Timisoara, Timisoara;*[(g)] *Faculty of Physics, University of Bucharest, Bucharest; Romania*
[28] [(a)] *Faculty of Mathematics, Physics and Informatics, Comenius University, Bratislava;*[(b)] *Department of Subnuclear Physics, Institute of Experimental Physics of the Slovak Academy of Sciences, Kosice; Slovak Republic*

JHEP01(2025)053

[29] Physics Department, Brookhaven National Laboratory, Upton NY; United States of America
[30] Universidad de Buenos Aires, Facultad de Ciencias Exactas y Naturales, Departamento de Física, y CONICET, Instituto de Física de Buenos Aires (IFIBA), Buenos Aires; Argentina
[31] California State University, CA; United States of America
[32] Cavendish Laboratory, University of Cambridge, Cambridge; United Kingdom
[33] [(a)] Department of Physics, University of Cape Town, Cape Town;[(b)] iThemba Labs, Western Cape;[(c)] Department of Mechanical Engineering Science, University of Johannesburg, Johannesburg;[(d)] National Institute of Physics, University of the Philippines Diliman (Philippines);[(e)] University of South Africa, Department of Physics, Pretoria;[(f)] University of Zululand, KwaDlangezwa;[(g)] School of Physics, University of the Witwatersrand, Johannesburg; South Africa
[34] Department of Physics, Carleton University, Ottawa ON; Canada
[35] [(a)] Faculté des Sciences Ain Chock, Université Hassan II de Casablanca;[(b)] Faculté des Sciences, Université Ibn-Tofail, Kénitra;[(c)] Faculté des Sciences Semlalia, Université Cadi Ayyad, LPHEA-Marrakech;[(d)] LPMR, Faculté des Sciences, Université Mohamed Premier, Oujda;[(e)] Faculté des sciences, Université Mohammed V, Rabat;[(f)] Institute of Applied Physics, Mohammed VI Polytechnic University, Ben Guerir; Morocco
[36] CERN, Geneva; Switzerland
[37] Affiliated with an institute covered by a cooperation agreement with CERN
[38] Affiliated with an international laboratory covered by a cooperation agreement with CERN
[39] Enrico Fermi Institute, University of Chicago, Chicago IL; United States of America
[40] LPC, Université Clermont Auvergne, CNRS/IN2P3, Clermont-Ferrand; France
[41] Nevis Laboratory, Columbia University, Irvington NY; United States of America
[42] Niels Bohr Institute, University of Copenhagen, Copenhagen; Denmark
[43] [(a)] Dipartimento di Fisica, Università della Calabria, Rende;[(b)] INFN Gruppo Collegato di Cosenza, Laboratori Nazionali di Frascati; Italy
[44] Physics Department, Southern Methodist University, Dallas TX; United States of America
[45] Physics Department, University of Texas at Dallas, Richardson TX; United States of America
[46] National Centre for Scientific Research "Demokritos", Agia Paraskevi; Greece
[47] [(a)] Department of Physics, Stockholm University;[(b)] Oskar Klein Centre, Stockholm; Sweden
[48] Deutsches Elektronen-Synchrotron DESY, Hamburg and Zeuthen; Germany
[49] Fakultät Physik, Technische Universität Dortmund, Dortmund; Germany
[50] Institut für Kern- und Teilchenphysik, Technische Universität Dresden, Dresden; Germany
[51] Department of Physics, Duke University, Durham NC; United States of America
[52] SUPA - School of Physics and Astronomy, University of Edinburgh, Edinburgh; United Kingdom
[53] INFN e Laboratori Nazionali di Frascati, Frascati; Italy
[54] Physikalisches Institut, Albert-Ludwigs-Universität Freiburg, Freiburg; Germany
[55] II. Physikalisches Institut, Georg-August-Universität Göttingen, Göttingen; Germany
[56] Département de Physique Nucléaire et Corpusculaire, Université de Genève, Genève; Switzerland
[57] [(a)] Dipartimento di Fisica, Università di Genova, Genova;[(b)] INFN Sezione di Genova; Italy
[58] II. Physikalisches Institut, Justus-Liebig-Universität Giessen, Giessen; Germany
[59] SUPA - School of Physics and Astronomy, University of Glasgow, Glasgow; United Kingdom
[60] LPSC, Université Grenoble Alpes, CNRS/IN2P3, Grenoble INP, Grenoble; France
[61] Laboratory for Particle Physics and Cosmology, Harvard University, Cambridge MA; United States of America
[62] [(a)] Department of Modern Physics and State Key Laboratory of Particle Detection and Electronics, University of Science and Technology of China, Hefei;[(b)] Institute of Frontier and Interdisciplinary Science and Key Laboratory of Particle Physics and Particle Irradiation (MOE), Shandong University, Qingdao;[(c)] School of Physics and Astronomy, Shanghai Jiao Tong University, Key Laboratory for Particle Astrophysics and Cosmology (MOE), SKLPPC, Shanghai;[(d)] Tsung-Dao Lee Institute, Shanghai;[(e)] School of Physics, Zhengzhou University; China
[63] [(a)] Kirchhoff-Institut für Physik, Ruprecht-Karls-Universität Heidelberg, Heidelberg;[(b)] Physikalisches Institut, Ruprecht-Karls-Universität Heidelberg, Heidelberg; Germany
[64] [(a)] Department of Physics, Chinese University of Hong Kong, Shatin, N.T., Hong Kong;[(b)] Department of Physics, University of Hong Kong, Hong Kong;[(c)] Department of Physics and Institute for Advanced Study,

Hong Kong University of Science and Technology, Clear Water Bay, Kowloon, Hong Kong; China
[65] Department of Physics, National Tsing Hua University, Hsinchu; Taiwan
[66] IJCLab, Université Paris-Saclay, CNRS/IN2P3, 91405, Orsay; France
[67] Centro Nacional de Microelectrónica (IMB-CNM-CSIC), Barcelona; Spain
[68] Department of Physics, Indiana University, Bloomington IN; United States of America
[69] [(a)] INFN Gruppo Collegato di Udine, Sezione di Trieste, Udine; [(b)] ICTP, Trieste; [(c)] Dipartimento Politecnico di Ingegneria e Architettura, Università di Udine, Udine; Italy
[70] [(a)] INFN Sezione di Lecce; [(b)] Dipartimento di Matematica e Fisica, Università del Salento, Lecce; Italy
[71] [(a)] INFN Sezione di Milano; [(b)] Dipartimento di Fisica, Università di Milano, Milano; Italy
[72] [(a)] INFN Sezione di Napoli; [(b)] Dipartimento di Fisica, Università di Napoli, Napoli; Italy
[73] [(a)] INFN Sezione di Pavia; [(b)] Dipartimento di Fisica, Università di Pavia, Pavia; Italy
[74] [(a)] INFN Sezione di Pisa; [(b)] Dipartimento di Fisica E. Fermi, Università di Pisa, Pisa; Italy
[75] [(a)] INFN Sezione di Roma; [(b)] Dipartimento di Fisica, Sapienza Università di Roma, Roma; Italy
[76] [(a)] INFN Sezione di Roma Tor Vergata; [(b)] Dipartimento di Fisica, Università di Roma Tor Vergata, Roma; Italy
[77] [(a)] INFN Sezione di Roma Tre; [(b)] Dipartimento di Matematica e Fisica, Università Roma Tre, Roma; Italy
[78] [(a)] INFN-TIFPA; [(b)] Università degli Studi di Trento, Trento; Italy
[79] Universität Innsbruck, Department of Astro and Particle Physics, Innsbruck; Austria
[80] University of Iowa, Iowa City IA; United States of America
[81] Department of Physics and Astronomy, Iowa State University, Ames IA; United States of America
[82] Istinye University, Sariyer, Istanbul; Türkiye
[83] [(a)] Departamento de Engenharia Elétrica, Universidade Federal de Juiz de Fora (UFJF), Juiz de Fora; [(b)] Universidade Federal do Rio De Janeiro COPPE/EE/IF, Rio de Janeiro; [(c)] Instituto de Física, Universidade de São Paulo, São Paulo; [(d)] Rio de Janeiro State University, Rio de Janeiro; Brazil
[84] KEK, High Energy Accelerator Research Organization, Tsukuba; Japan
[85] Graduate School of Science, Kobe University, Kobe; Japan
[86] [(a)] AGH University of Krakow, Faculty of Physics and Applied Computer Science, Krakow; [(b)] Marian Smoluchowski Institute of Physics, Jagiellonian University, Krakow; Poland
[87] Institute of Nuclear Physics Polish Academy of Sciences, Krakow; Poland
[88] Faculty of Science, Kyoto University, Kyoto; Japan
[89] Research Center for Advanced Particle Physics and Department of Physics, Kyushu University, Fukuoka; Japan
[90] Instituto de Física La Plata, Universidad Nacional de La Plata and CONICET, La Plata; Argentina
[91] Physics Department, Lancaster University, Lancaster; United Kingdom
[92] Oliver Lodge Laboratory, University of Liverpool, Liverpool; United Kingdom
[93] Department of Experimental Particle Physics, Jožef Stefan Institute and Department of Physics, University of Ljubljana, Ljubljana; Slovenia
[94] School of Physics and Astronomy, Queen Mary University of London, London; United Kingdom
[95] Department of Physics, Royal Holloway University of London, Egham; United Kingdom
[96] Department of Physics and Astronomy, University College London, London; United Kingdom
[97] Louisiana Tech University, Ruston LA; United States of America
[98] Fysiska institutionen, Lunds universitet, Lund; Sweden
[99] Departamento de Física Teorica C-15 and CIAFF, Universidad Autónoma de Madrid, Madrid; Spain
[100] Institut für Physik, Universität Mainz, Mainz; Germany
[101] School of Physics and Astronomy, University of Manchester, Manchester; United Kingdom
[102] CPPM, Aix-Marseille Université, CNRS/IN2P3, Marseille; France
[103] Department of Physics, University of Massachusetts, Amherst MA; United States of America
[104] Department of Physics, McGill University, Montreal QC; Canada
[105] School of Physics, University of Melbourne, Victoria; Australia
[106] Department of Physics, University of Michigan, Ann Arbor MI; United States of America
[107] Department of Physics and Astronomy, Michigan State University, East Lansing MI; United States of America
[108] Group of Particle Physics, University of Montreal, Montreal QC; Canada

JHEP01(2025)053

[109] *Fakultät für Physik, Ludwig-Maximilians-Universität München, München; Germany*
[110] *Max-Planck-Institut für Physik (Werner-Heisenberg-Institut), München; Germany*
[111] *Graduate School of Science and Kobayashi-Maskawa Institute, Nagoya University, Nagoya; Japan*
[112] *Department of Physics and Astronomy, University of New Mexico, Albuquerque NM; United States of America*
[113] *Institute for Mathematics, Astrophysics and Particle Physics, Radboud University/Nikhef, Nijmegen; Netherlands*
[114] *Nikhef National Institute for Subatomic Physics and University of Amsterdam, Amsterdam; Netherlands*
[115] *Department of Physics, Northern Illinois University, DeKalb IL; United States of America*
[116] *[(a)] New York University Abu Dhabi, Abu Dhabi;[(b)] United Arab Emirates University, Al Ain; United Arab Emirates*
[117] *Department of Physics, New York University, New York NY; United States of America*
[118] *Ochanomizu University, Otsuka, Bunkyo-ku, Tokyo; Japan*
[119] *Ohio State University, Columbus OH; United States of America*
[120] *Homer L. Dodge Department of Physics and Astronomy, University of Oklahoma, Norman OK; United States of America*
[121] *Department of Physics, Oklahoma State University, Stillwater OK; United States of America*
[122] *Palacký University, Joint Laboratory of Optics, Olomouc; Czech Republic*
[123] *Institute for Fundamental Science, University of Oregon, Eugene, OR; United States of America*
[124] *Graduate School of Science, Osaka University, Osaka; Japan*
[125] *Department of Physics, University of Oslo, Oslo; Norway*
[126] *Department of Physics, Oxford University, Oxford; United Kingdom*
[127] *LPNHE, Sorbonne Université, Université Paris Cité, CNRS/IN2P3, Paris; France*
[128] *Department of Physics, University of Pennsylvania, Philadelphia PA; United States of America*
[129] *Department of Physics and Astronomy, University of Pittsburgh, Pittsburgh PA; United States of America*
[130] *[(a)] Laboratório de Instrumentação e Física Experimental de Partículas - LIP, Lisboa;[(b)] Departamento de Física, Faculdade de Ciências, Universidade de Lisboa, Lisboa;[(c)] Departamento de Física, Universidade de Coimbra, Coimbra;[(d)] Centro de Física Nuclear da Universidade de Lisboa, Lisboa;[(e)] Departamento de Física, Universidade do Minho, Braga;[(f)] Departamento de Física Teórica y del Cosmos, Universidad de Granada, Granada (Spain);[(g)] Departamento de Física, Instituto Superior Técnico, Universidade de Lisboa, Lisboa; Portugal*
[131] *Institute of Physics of the Czech Academy of Sciences, Prague; Czech Republic*
[132] *Czech Technical University in Prague, Prague; Czech Republic*
[133] *Charles University, Faculty of Mathematics and Physics, Prague; Czech Republic*
[134] *Particle Physics Department, Rutherford Appleton Laboratory, Didcot; United Kingdom*
[135] *IRFU, CEA, Université Paris-Saclay, Gif-sur-Yvette; France*
[136] *Santa Cruz Institute for Particle Physics, University of California Santa Cruz, Santa Cruz CA; United States of America*
[137] *[(a)] Departamento de Física, Pontificia Universidad Católica de Chile, Santiago;[(b)] Millennium Institute for Subatomic physics at high energy frontier (SAPHIR), Santiago;[(c)] Instituto de Investigación Multidisciplinario en Ciencia y Tecnología, y Departamento de Física, Universidad de La Serena;[(d)] Universidad Andres Bello, Department of Physics, Santiago;[(e)] Instituto de Alta Investigación, Universidad de Tarapacá, Arica;[(f)] Departamento de Física, Universidad Técnica Federico Santa María, Valparaíso; Chile*
[138] *Department of Physics, Institute of Science, Tokyo; Japan*
[139] *Department of Physics, University of Washington, Seattle WA; United States of America*
[140] *Department of Physics and Astronomy, University of Sheffield, Sheffield; United Kingdom*
[141] *Department of Physics, Shinshu University, Nagano; Japan*
[142] *Department Physik, Universität Siegen, Siegen; Germany*
[143] *Department of Physics, Simon Fraser University, Burnaby BC; Canada*
[144] *SLAC National Accelerator Laboratory, Stanford CA; United States of America*
[145] *Department of Physics, Royal Institute of Technology, Stockholm; Sweden*
[146] *Departments of Physics and Astronomy, Stony Brook University, Stony Brook NY; United States of*

America
[147] Department of Physics and Astronomy, University of Sussex, Brighton; United Kingdom
[148] School of Physics, University of Sydney, Sydney; Australia
[149] Institute of Physics, Academia Sinica, Taipei; Taiwan
[150] [(a)] E. Andronikashvili Institute of Physics, Iv. Javakhishvili Tbilisi State University, Tbilisi;[(b)] High Energy Physics Institute, Tbilisi State University, Tbilisi;[(c)] University of Georgia, Tbilisi; Georgia
[151] Department of Physics, Technion, Israel Institute of Technology, Haifa; Israel
[152] Raymond and Beverly Sackler School of Physics and Astronomy, Tel Aviv University, Tel Aviv; Israel
[153] Department of Physics, Aristotle University of Thessaloniki, Thessaloniki; Greece
[154] International Center for Elementary Particle Physics and Department of Physics, University of Tokyo, Tokyo; Japan
[155] Department of Physics, University of Toronto, Toronto ON; Canada
[156] [(a)] TRIUMF, Vancouver BC;[(b)] Department of Physics and Astronomy, York University, Toronto ON; Canada
[157] Division of Physics and Tomonaga Center for the History of the Universe, Faculty of Pure and Applied Sciences, University of Tsukuba, Tsukuba; Japan
[158] Department of Physics and Astronomy, Tufts University, Medford MA; United States of America
[159] Department of Physics and Astronomy, University of California Irvine, Irvine CA; United States of America
[160] University of Sharjah, Sharjah; United Arab Emirates
[161] Department of Physics and Astronomy, University of Uppsala, Uppsala; Sweden
[162] Department of Physics, University of Illinois, Urbana IL; United States of America
[163] Instituto de Física Corpuscular (IFIC), Centro Mixto Universidad de Valencia - CSIC, Valencia; Spain
[164] Department of Physics, University of British Columbia, Vancouver BC; Canada
[165] Department of Physics and Astronomy, University of Victoria, Victoria BC; Canada
[166] Fakultät für Physik und Astronomie, Julius-Maximilians-Universität Würzburg, Würzburg; Germany
[167] Department of Physics, University of Warwick, Coventry; United Kingdom
[168] Waseda University, Tokyo; Japan
[169] Department of Particle Physics and Astrophysics, Weizmann Institute of Science, Rehovot; Israel
[170] Department of Physics, University of Wisconsin, Madison WI; United States of America
[171] Fakultät für Mathematik und Naturwissenschaften, Fachgruppe Physik, Bergische Universität Wuppertal, Wuppertal; Germany
[172] Department of Physics, Yale University, New Haven CT; United States of America

[a] Also Affiliated with an institute covered by a cooperation agreement with CERN
[b] Also at An-Najah National University, Nablus; Palestine
[c] Also at Borough of Manhattan Community College, City University of New York, New York NY; United States of America
[d] Also at Center for High Energy Physics, Peking University; China
[e] Also at Center for Interdisciplinary Research and Innovation (CIRI-AUTH), Thessaloniki; Greece
[f] Also at Centro Studi e Ricerche Enrico Fermi; Italy
[g] Also at CERN, Geneva; Switzerland
[h] Also at Département de Physique Nucléaire et Corpusculaire, Université de Genève, Genève; Switzerland
[i] Also at Departament de Fisica de la Universitat Autonoma de Barcelona, Barcelona; Spain
[j] Also at Department of Financial and Management Engineering, University of the Aegean, Chios; Greece
[k] Also at Department of Physics, Ben Gurion University of the Negev, Beer Sheva; Israel
[l] Also at Department of Physics, California State University, Sacramento; United States of America
[m] Also at Department of Physics, King's College London, London; United Kingdom
[n] Also at Department of Physics, Stanford University, Stanford CA; United States of America
[o] Also at Department of Physics, Stellenbosch University; South Africa
[p] Also at Department of Physics, University of Fribourg, Fribourg; Switzerland
[q] Also at Department of Physics, University of Thessaly; Greece
[r] Also at Department of Physics, Westmont College, Santa Barbara; United States of America
[s] Also at Faculty of Physics, Sofia University, 'St. Kliment Ohridski', Sofia; Bulgaria

[t] Also at Hellenic Open University, Patras; Greece
[u] Also at Institucio Catalana de Recerca i Estudis Avancats, ICREA, Barcelona; Spain
[v] Also at Institut für Experimentalphysik, Universität Hamburg, Hamburg; Germany
[w] Also at Institute for Nuclear Research and Nuclear Energy (INRNE) of the Bulgarian Academy of Sciences, Sofia; Bulgaria
[x] Also at Institute of Applied Physics, Mohammed VI Polytechnic University, Ben Guerir; Morocco
[y] Also at Institute of Particle Physics (IPP); Canada
[z] Also at Institute of Physics and Technology, Mongolian Academy of Sciences, Ulaanbaatar; Mongolia
[aa] Also at Institute of Physics, Azerbaijan Academy of Sciences, Baku; Azerbaijan
[ab] Also at Institute of Theoretical Physics, Ilia State University, Tbilisi; Georgia
[ac] Also at L2IT, Université de Toulouse, CNRS/IN2P3, UPS, Toulouse; France
[ad] Also at Lawrence Livermore National Laboratory, Livermore; United States of America
[ae] Also at National Institute of Physics, University of the Philippines Diliman (Philippines); Philippines
[af] Also at Technical University of Munich, Munich; Germany
[ag] Also at The Collaborative Innovation Center of Quantum Matter (CICQM), Beijing; China
[ah] Also at TRIUMF, Vancouver BC; Canada
[ai] Also at Università di Napoli Parthenope, Napoli; Italy
[aj] Also at University of Chinese Academy of Sciences (UCAS), Beijing; China
[ak] Also at University of Colorado Boulder, Department of Physics, Colorado; United States of America
[al] Also at Washington College, Chestertown, MD; United States of America
[am] Also at Yeditepe University, Physics Department, Istanbul; Türkiye
[*] Deceased

JHEP01(2025)053